Molecular and Cellular Mechanisms of Increased Angiogenesis in Multiple Myeloma: A Role for CXCL12

Sally K. Martin

Myeloma Research Group
Bone and Cancer Research Laboratory,
Division of Haematology,
Hanson Institute
Institute of Medical and Veterinary Science

&

Department of Medicine,
Faculty of Health Sciences
University of Adelaide

A thesis submitted to the University of Adelaide
for the degree of Doctor of Philosophy
December 2008

Chapter 3:

THE ROLE OF CXCL12 ON ANGIOGENESIS IN MULTIPLE MYELOMA

3.1 Introduction

Due to the absolute necessity of oxygen for cell survival, metabolism and growth, all mammalian cells are located within 100 - 200μm of a blood vessel, a distance which corresponds to the diffusion limit for oxygen through tissue [59]. While the establishment of the vascular network generally occurs during embryogenesis, on-going requirements for vascular expansion and pruning continue throughout adult life in processes such as wound healing, inflammation and female reproductive function [14,61,63]. Many of these requirements are fulfilled by a remodelling process known as angiogenesis. Angiogenesis is a complex, tightly-coordinated process in which new blood vessels are created through the sprouting or invagination of pre-existing vasculature [64,74].

It is well established that angiogenesis is also a key feature of tumorigenesis and is associated with a poor clinical outcome [91,92]. The acquisition of an angiogenic phenotype, induced by selective pressures and cumulative genetic alterations, facilitates the transition of a growth-restricted tumour to an active, invasive tumour. Tumour angiogenesis provides an increased supply of oxygen, nutrients and pro-survival factors to proliferating cancer cells, a system for the removal of waste products and a vascular route for tumour spread to secondary sites. In addition, growth factors released from the endothelium in response to tumour cells stimulate further tumour proliferation and migration. Angiogenesis is associated with the progression of many human tumours, including breast cancer [94-97], rectal carcinoma [98], prostate cancer [99], melanoma [100], and hepatocellular carcinoma [101-104]. More recently, angiogenesis has been shown to be involved with the progression of haematological malignancies such as ALL [105-107], AML [105,108,109], CML [105,110], CLL [111], MDS [112], NHL [113,134] and MM [4,6-8,116,412,413].

Morphologically, the BM microvasculature in biopsies from MM patients is tortuous and thin [4], mirroring the classical features of tumour angiogenesis in solid malignancies [88,89]. In MM, BM angiogenesis is associated with BM PC infiltration (defined as the percentage of MM PCs in the BM) [115,116], PC labelling index [6], elevated serum β2M levels [115,116] and overall patient survival [6-8].

The molecular mechanisms underlying the increased angiogenesis in MM are complex. Numerous autocrine and paracrine interactions between tumour cells and stromal cells within the BM microenvironment stimulate the secretion of chemokines, cytokines, growth

factors and MMPs which collectively orchestrate angiogenesis. Due to their ability to induce both EC migration and proliferation, chemokines are ideal regulators of angiogenesis [414]. Studies have shown that CXCR4 is the predominant CXC chemokine receptor expressed by ECs, and that CXCL12 is a potent EC chemoattractant [10,177,178]. Consistent with these findings, defective vascularisation is a common phenotype of both CXCR4 and CXCL12 knockout mice [173,207,208]. The CXCL12/CXCR4 chemokine axis has also been implicated in tumour angiogenesis *in vivo* [10,12,242,247,253]. Interestingly, in addition to their own direct effects on ECs, angiogenic factors such as VEGF and bFGF can also increase CXCL12 and/or CXCR4 expression in ECs and thereby potentiate the angiogenic actions of CXCL12 [10,12,14,254].

CXCL12 is highly expressed by MM PCs [9], and circulating levels of CXCL12 are elevated in the BM [263] and peripheral blood (PB) circulation [9] of MM patients compared with age-matched normal donors and MGUS patients. In addition, CXCR4 is the predominant chemokine receptor expressed by MM PCs [261,262]. The CXCL12/CXCR4 axis is crucial for several aspects of MM progression, including the transendothelial migration of MM PCs into the BM [164,264,265], MM PC migration and retention within the BM, in close proximity to stromal cells [168,192,260,266,267] and osteoclastic bone resorption [9].

To date, the contribution of CXCL12 to the increased BM angiogenesis seen in MM patients has not been examined. In this chapter, bone trephine specimens were collected from newly-diagnosed patients with MM and MGUS and used to examine whether there is any association between BM PC burden, BM angiogenesis, and circulating PB levels of CXCL12 in MM patients. In addition, conditioned media from the MM PC line, RPMI-8226, was used to examine whether MM PC-derived CXCL12 stimulates *in vitro* angiogenesis.

3.2 Results

3.2.1 Patient Studies

3.2.1.1 Bone marrow microvessel density is elevated in MM patients and correlates with plasma cell burden.

To investigate whether BM MVD, a surrogate marker of angiogenesis, is elevated in MM patients and is associated with disease progression, MVD analysis was performed on biopsy samples from a cohort of individuals diagnosed at different stages of the disease spectrum. Sections of paraffin-embedded trephine biopsies from previously untreated MM (n=41) and MGUS (n=25) patients and haematologically normal individuals (n=17) were stained with an EC-reactive anti-CD34 antibody and MVD analysis performed as described in the Materials and Methods (see Section 2.3.10.1). To eliminate age-related bias, normal subjects and MGUS patients were approximately age-matched with MM patients and the average ages of each patient group was 62, 67 and 67 years respectively (see Table 3.1).

Figure 3.1 displays representative CD34 staining of bone trephine sections taken from a haematologically normal subject and a MM patient with extensive MM PC infiltration. All sections were counterstained with haematoxylin, and the obvious uniformity of the haematoxylin-stained nuclei throughout the MM trephine specimen (Figure 3.1B) reflects the uncontrolled expansion of MM PCs which has displaced normal haemopoietic cells. The large round white areas represent fat deposits within the bone trephine. Importantly, a noticeable increase in the number of microvessels, stained red with the EC-reactive CD34 antibody (highlighted by arrows), was observed in bone trephine specimens from MM patients compared to haematologically normal subjects.

Two established protocols have been described for MVD assessment in BM trephines. The first method, often referred to as the "hot spot" method, involves the assessment of BM MVD in three areas displaying the highest vascularity [6,117,404-406]. The second method involves the assessment of BM MVD across the entire biopsy specimen [8,84,106,134,407,408].

To examine whether there was any difference in our cohort of patient trephine specimens, BM MVD was assessed by both methods. When the "hot spot" MVD measurement for each patient was plotted with reference to their "whole trephine" MVD measurement, a statistically significant correlation was observed (Figure 3.2, $p<0.001$, Pearson Product

Table 3.1. Patient and control subject information

	No. of Subjects	Mean Age (Range)	Male / Female	Mean MM PC Burden (Range)	Mean CXCL12 Conc. ± SEM (No. of Subjects*)	Mean MVD: whole (Range) (No. of subjects^)	Mean MVD: "hot spot" (Range) (No. of subjects^)
Normal	40	62 (42 - 86)	24 / 16	0.8% (0 - 6%)	2187 ± 74 pg/mL (n=29)	23.0 (5.2 - 51.3) (n=17)	29.7 (9.0 - 53.0) (n=17)
MGUS	37	67 (45 - 83)	22 / 15	4.4% (1 - 10%)	2583 ± 106 pg/mL (n=25)	26.3 (13.7 - 61.1) (n=25)	35.1 (17.0 - 63.0) (n=25)
MM	67	67 (44 - 84)	37 / 30	31.5% (8 - 81%)	2952 ± 116 pg/mL (n=62)	57.4 (22.8 - 121.6) (n=41)	71.4 (32.0 - 168.3) (n=41)

* Due to the lack of availability of suitable PB plasma samples, CXCL12 levels were only measured in the indicated number of patient samples.

^ Due to the lack of availability of suitable BM trephine specimens, BM MVD analyses were only performed on the indicated number of patient samples.

Figure 3.1. Immunohistochemical Microvessel Staining of Patient Bone Marrow Trephine Specimens. Anti-CD34 endothelial staining of blood vessels (see arrows) were performed on sections of paraffin-embedded trephine specimens derived from the iliac crest of (**A**) age-matched haematologically normal donors and (**B**) MM patients at the time of diagnosis. Sections were counterstained with haematoxylin. Areas of white represent adipocytes within the trephine specimen. An increase in bone marrow microvessel density was consistently observed in trephine specimens collected from MM patients compared to haematologically normal individuals. Images were taken at x200 magnification.

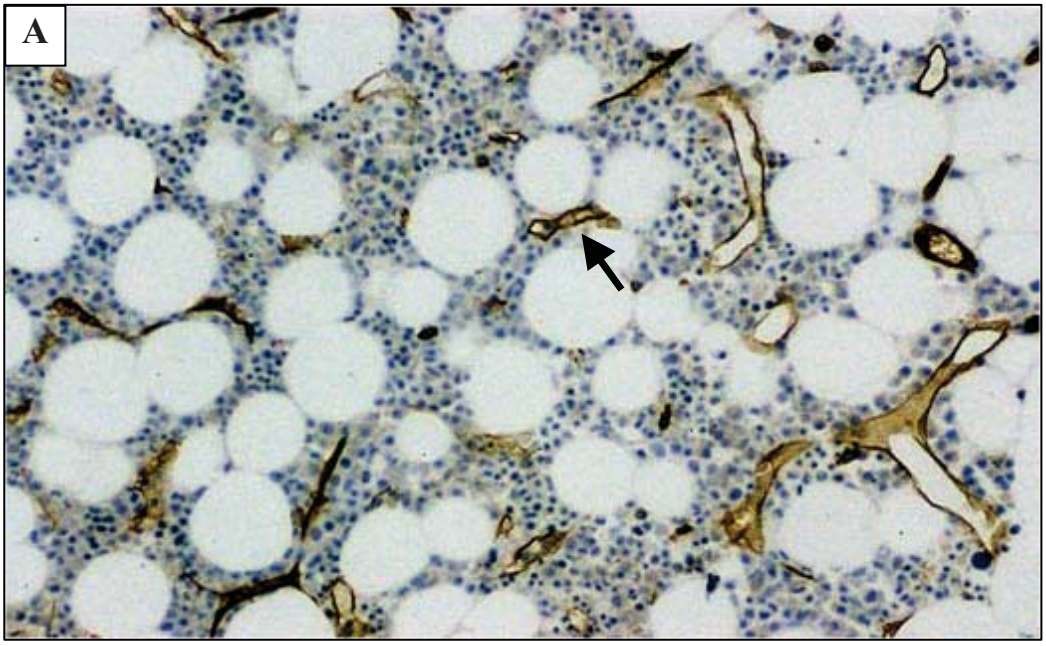
A

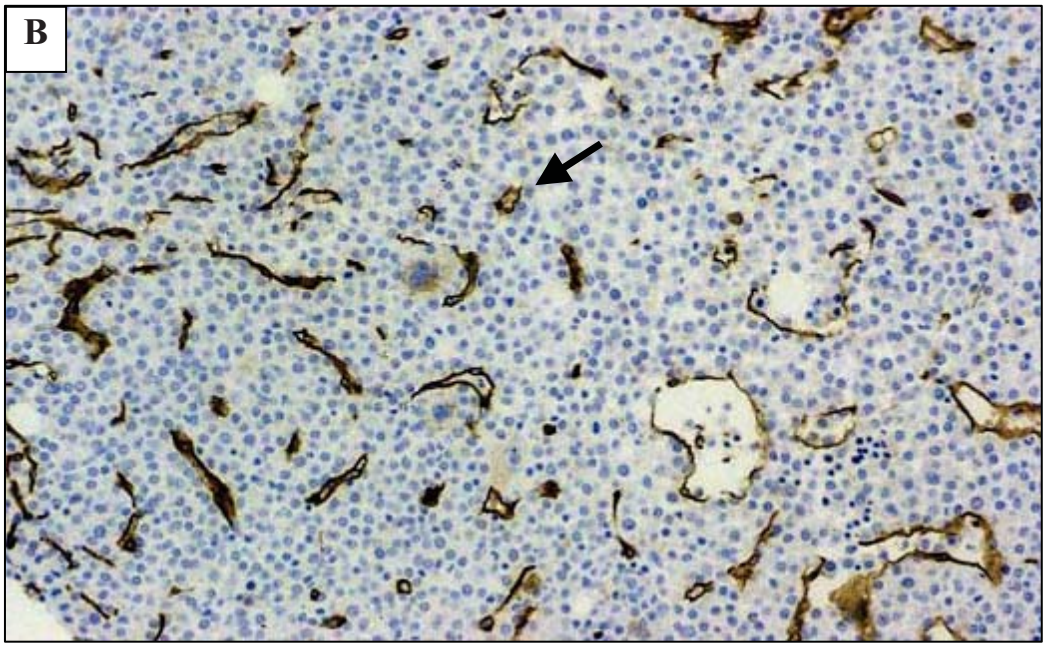
B

Figure 3.2. A Comparison Between Two Established Methods of Assessing Bone Marrow Microvessel Density. Where suitable bone marrow trephine specimens were available, paraffin-embedded sections were stained with an endothelial cell-reactive monoclonal antibody to CD34 (see Figure 3.1). Bone marrow microvessel density was assessed across the entire biopsy specimen or at three "hot spots" displaying the highest vascularity (see Section 2.3.10.1, Materials and Methods). In this study, microvessel density analysis was performed on specimens collected from haematologically normal patients (● , n=17), MGUS patients (●, n=25) and MM patients (● , n=41) at the time of diagnosis, prior to treatment. A statistically significant correlation was found between the two established methods of assessing bone marrow microvessel density in these patients ($p<0.001$, Pearson Product Moment).

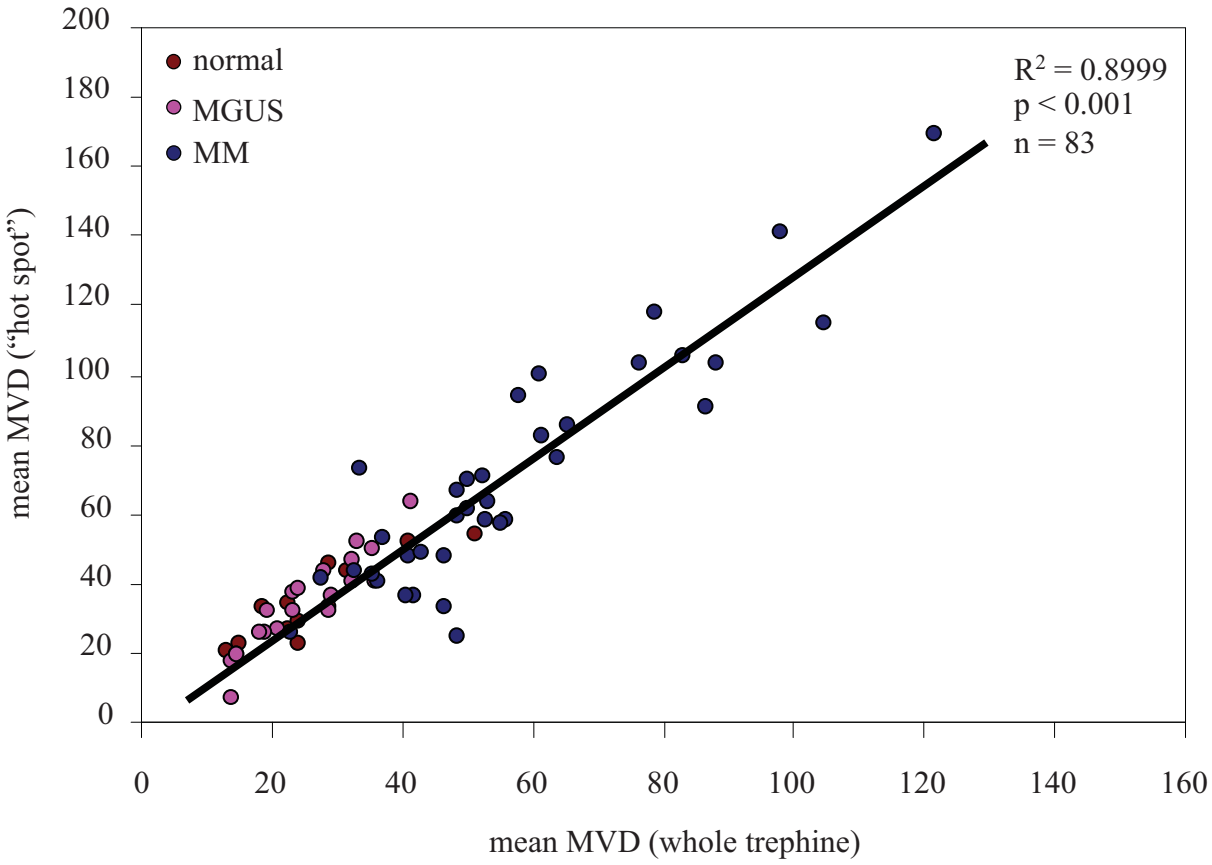
normal
MGUS
MM
$R^2 = 0.8999$
$p < 0.001$
$n = 83$
mean MVD ("hot spot")
mean MVD (whole trephine)
0
20
40
60
80
100
120
140
160
180
200

Moment). As no difference between the two methods of BM MVD assessment was evident, the "whole trephine" method was used for all studies described hereafter.

When the MVD measurement for each haematologically normal subject, MGUS and MM patient was graphed together in their respective patient groups, BM MVD was significantly higher in the MM patient cohort compared to both the normal and MGUS groups (Figure 3.3A, $p<0.001$, one-way ANOVA). In contrast, no significant difference in BM MVD was observed between the haematologically normal and MGUS patient cohorts ($p=0.332$, one-way ANOVA). To better illustrate the differences in the overall average BM MVD between these patient groups, the same data were re-plotted as a bar graph (Figure 3.3B). BM trephine biopsies from haematologically normal individuals contained an average BM MVD measurement of 23 ± 2.76 vessels/ high powered field of view (hpf), and MGUS patient specimens contained an average of 26.3 ± 2.11 vessels/ hpf. Importantly, MM patient BM trephines contained an average of 57.4 ± 3.4 vessels/ hpf which, as mentioned previously, was significantly higher than both the normal and MGUS patient groups (Figure 3.3B, $p<0.001$, one-way ANOVA).

Given that the presence of malignant MM PCs is associated with the increased BM MVD observed in MM patients, we next examined whether there was a direct relationship between the degree of tumour burden, defined as the percentage of MM PCs present in the BM, and the level of BM angiogenesis observed in these patients. Where suitable data was available, the BM MVD measurement for MM (n=40) and MGUS (n=24) patients were plotted with reference to their respective BM PC burden, as assessed by a clinical haematologist during routine diagnostic tests at the time each trephine biopsy was performed. A statistically significant association between BM MVD and BM PC burden was observed in these MM and MGUS patients (Figure 3.4, $p<0.00001$, Pearson Product Moment). Haematologically normal individuals were not included in this assessment because malignant PCs are not present in sufficient numbers in the BM of these subjects.

3.2.1.2 Circulating levels of CXCL12 are elevated in MM patients and correlate with BM plasma cell burden and MVD.

In the normal BM environment, CXCL12 is expressed by a number of different cells including OBs lining endosteal surfaces [215,415,416], BMSCs [415], and vascular ECs [415]. To examine whether CXCL12 is expressed by MM PCs, sections of paraffin-embedded

Figure 3.3. Bone Marrow Microvessel Density Correlates with Patient Disease Status and is Elevated in MM Patients. Where suitable bone marrow trephine specimens were available, microvessel density analysis was performed on paraffin-embedded trephine biopsy specimens stained with an endothelial cell-reactive monoclonal antibody to CD34 (see Figure 3.1). In this study, microvessel density analysis was performed on haematologically normal patients (n=17), MGUS patients (n=25) and MM patients (n=41) at the time of diagnosis, prior to treatment. In (**A**), the mean microvessel density for individual patients within the MM, MGUS and control groups is plotted as a dot to illustrate the range in microvessel density observed within each group. In (**B**), the average microvessel density for all subjects within each patient group is plotted to illustrate the overall trend in microvessel density between patient groups. Error bars represent the standard error within each cohort of patients. Bone marrow microvessel density was significantly higher in MM patients compared to the both the control and MGUS groups ($p<0.001$, one-way ANOVA). No significant difference in microvessel density was observed between the control and MGUS groups ($p=0.33$, one-way ANOVA).

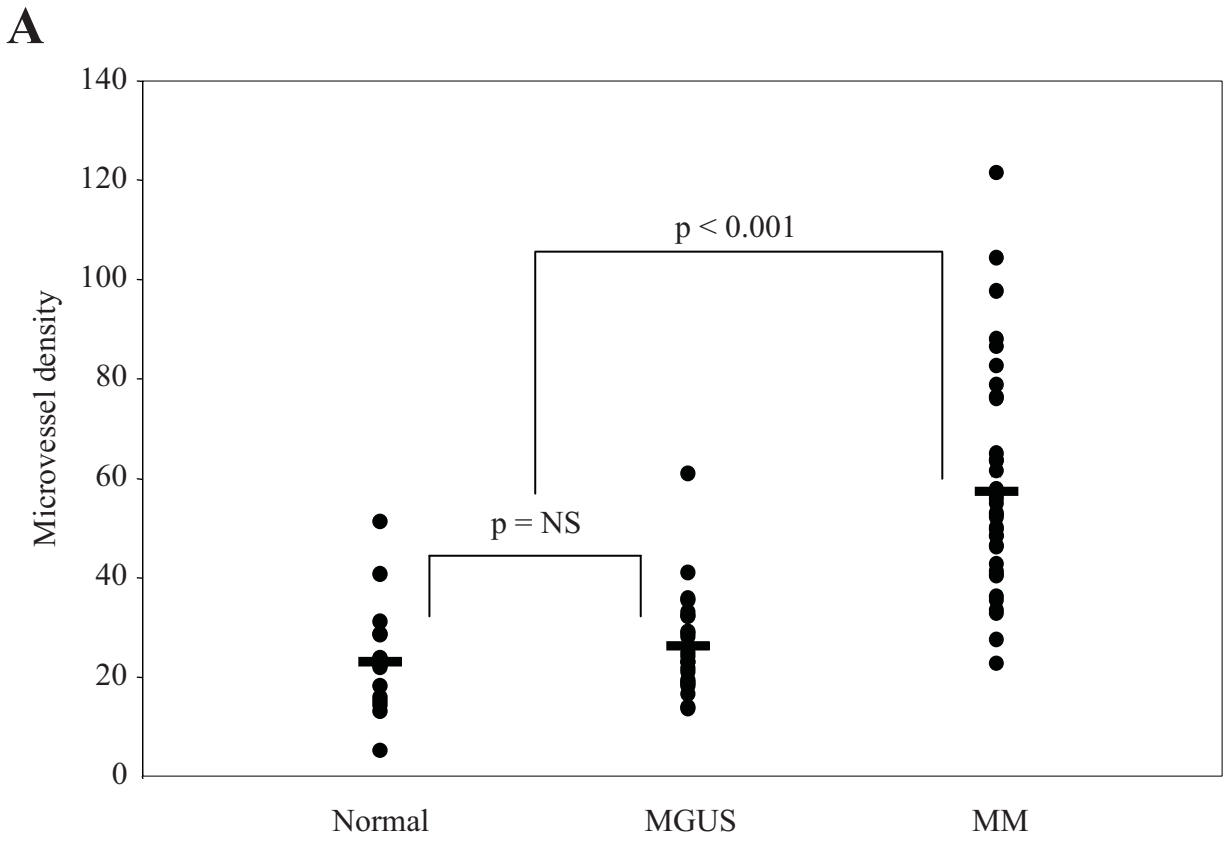
A
140
120
100
80
60
40
20
0
Microvessel density
p < 0.001
p = NS
Normal
MGUS
MM

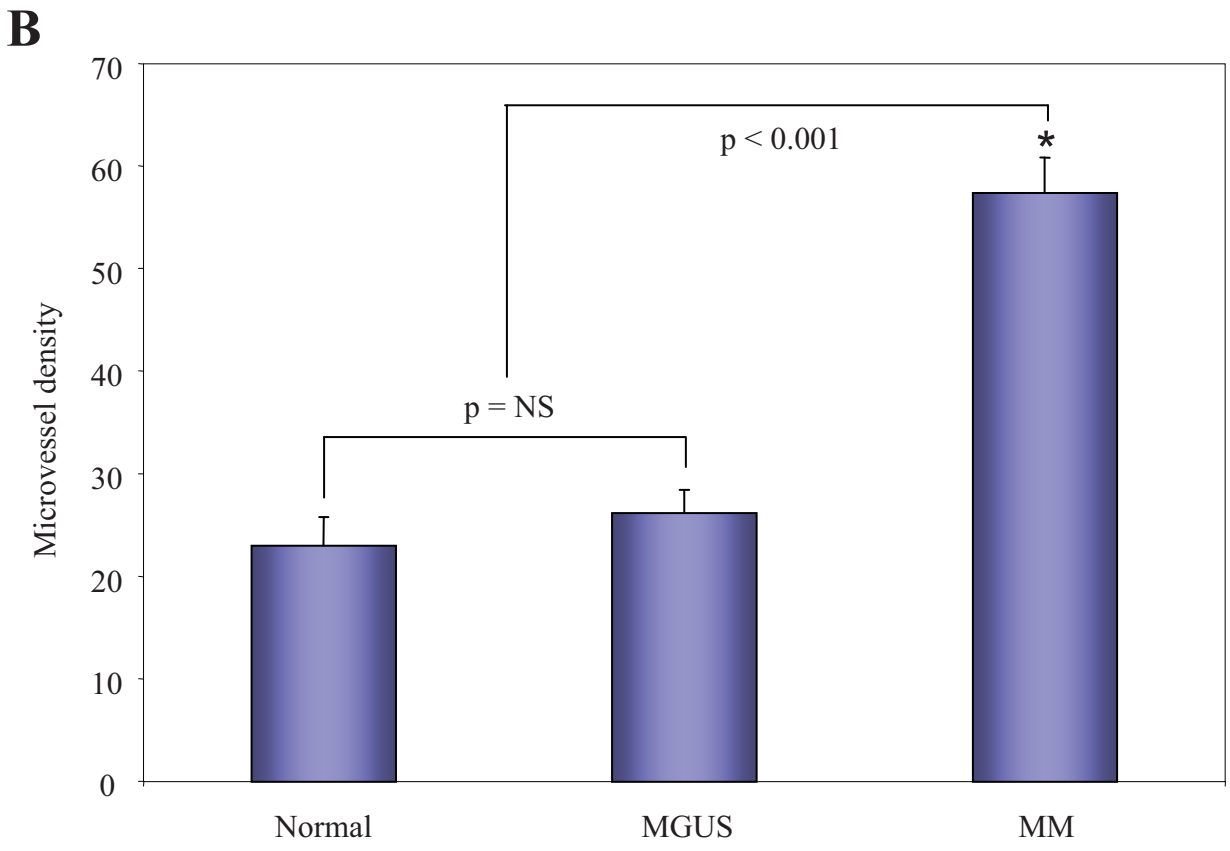
B
70
60
50
40
30
20
10
0
Microvessel density
p < 0.001
*
p = NS
Normal
MGUS
MM

Figure 3.4. Bone Marrow Plasma Cell Burden Correlates with Microvessel Density in MM and MGUS Patients. Where suitable bone marrow trephine specimens were available, microvessel density data were collected from MM (● , n=40) and MGUS (● , n=24) patients at diagnosis and plotted with reference to their respective bone marrow plasma cell burden, as assessed by a haematologist. Haematologically normal individuals were not included in this assessment because malignant PCs are not present in sufficient numbers in the BM of these subjects. Increasing bone marrow microvessel density was observed with increasing plasma cell burden in MM and MGUS patients and this correlation was statistically significant ($p<0.00001$, Pearson Product Moment).

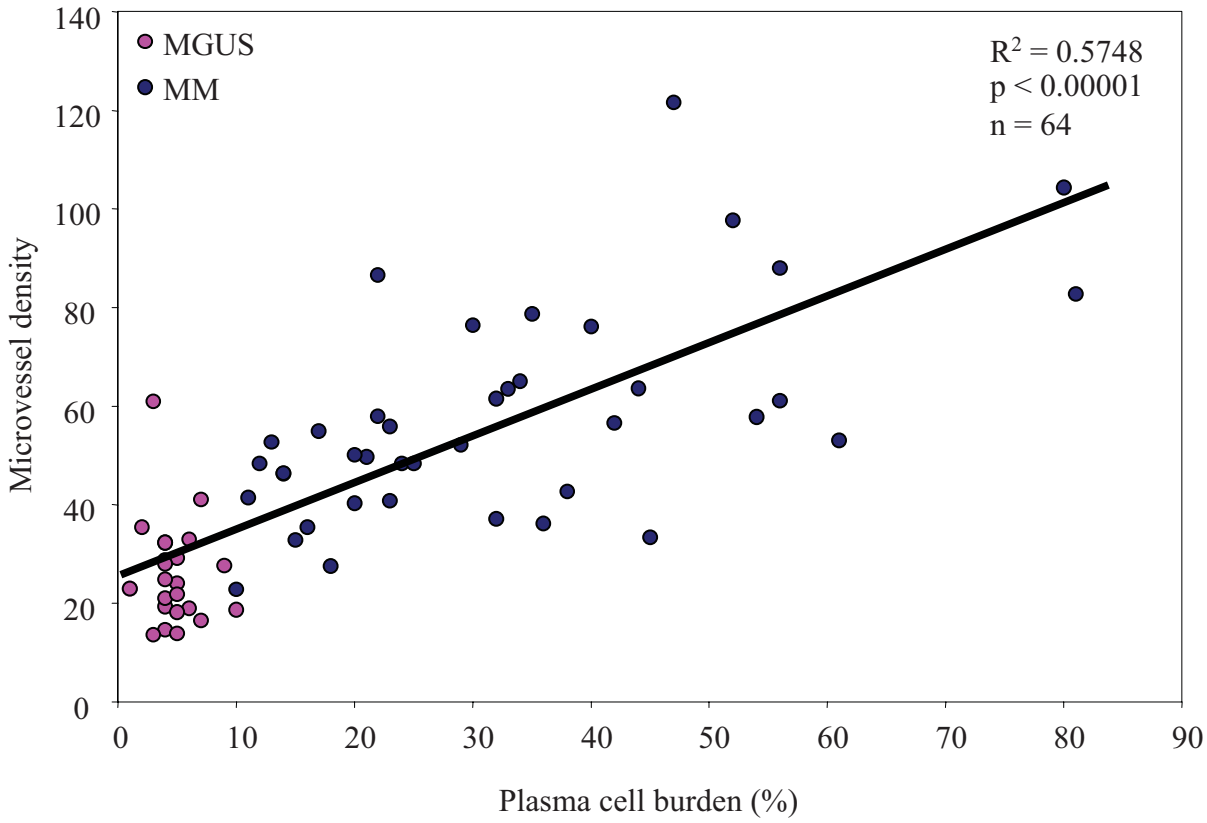
MGUS
MM
$R^2 = 0.5748$
$p < 0.00001$
$n = 64$
Microvessel density
Plasma cell burden (%)
0
20
40
60
80
100
120
140
0
10
20
30
40
50
60
70
80
90

trephine biopsies from our cohort of haematologically normal individuals, and MGUS and MM patients were stained with an anti-CXCL12 antibody to detect CXCL12 protein expression using immunohistochemistry. Figure 3.5 displays representative examples of CXCL12 staining in trephine biopsies taken from a haematologically normal individual, and three representative MM patients. All sections were counterstained with haematoxylin, and the large round white areas represent fat deposits within the trephine. As highlighted by arrows, CXCL12 is expressed by EC and BMSCs in these samples. Importantly, malignant MM PCs were found to represent a major source of CXCL12 protein in the BM microenvironment in MM patients.

To determine whether the aberrant expression of CXCL12 by MM PCs affects circulating levels of CXCL12 in patients, PB plasma samples collected from our age-matched cohort of patients were analysed for levels of CXCL12 using a commercial ELISA kit. When the circulating CXCL12 concentration from each haematologically normal individual (n=29), MGUS patient (n=25) and MM patient (n=62) were graphed together in their respective patient groups, circulating PB levels of CXCL12 were found to be significantly higher in the MM patient group compared to the MGUS and healthy patient groups (Figure 3.6A, $p<0.001$, one-way ANOVA). While an increase in circulating levels of CXCL12 was observed between the MGUS and MM patient groups, this was not statistically significant ($p=0.16$, Mann-Whitney Rank Sum). Similarly, whilst an increase in circulating levels of CXCL12 was also observed between control and MGUS groups, statistical significance was not achieved ($p=0.06$, one-way ANOVA).

To better illustrate the differences in the overall average circulating CXCL12 levels between these patient groups, the same data were re-plotted as a bar graph (Figure 3.6B). Circulating CXCL12 levels in PB plasma samples from haematologically normal individuals and MGUS patients were 2187 ± 74pg/mL and 2583 ± 106pg/mL, respectively. Importantly, an average circulating CXCL12 concentration of 2952 ± 116pg/mL was observed in the MM patient group (Figure 3.6B, $p<0.001$, one-way ANOVA).

3.2.1.3 Circulating CXCL12 levels in MM and MGUS patients correlate with BM plasma cell burden and MVD.

Having identified MM PCs as a major source of CXCL12 in the BM microenvironment of MM patients (see Figure 3.5), we next examined whether there was a direct relationship

Figure 3.5. Immunohistochemical CXCL12 Staining of Patient Bone Marrow Trephines. CXCL12 immunohistochemical staining was performed on sections of paraffin-embedded trephine specimens derived from the iliac crest of (**A**) age-matched normal donors, or (**B - D**) MM patients at the time of diagnosis. All sections were counterstained with haematoxylin. Areas of white represent adipocytes within the trephine specimen. Large vascular structures stained positive for CXCL12 (arrows), and in MM specimens, identifiable myeloma plasma cell nests were found to express appreciable levels of CXCL12 protein (circled). Images were taken at x200 and x40 magnification.

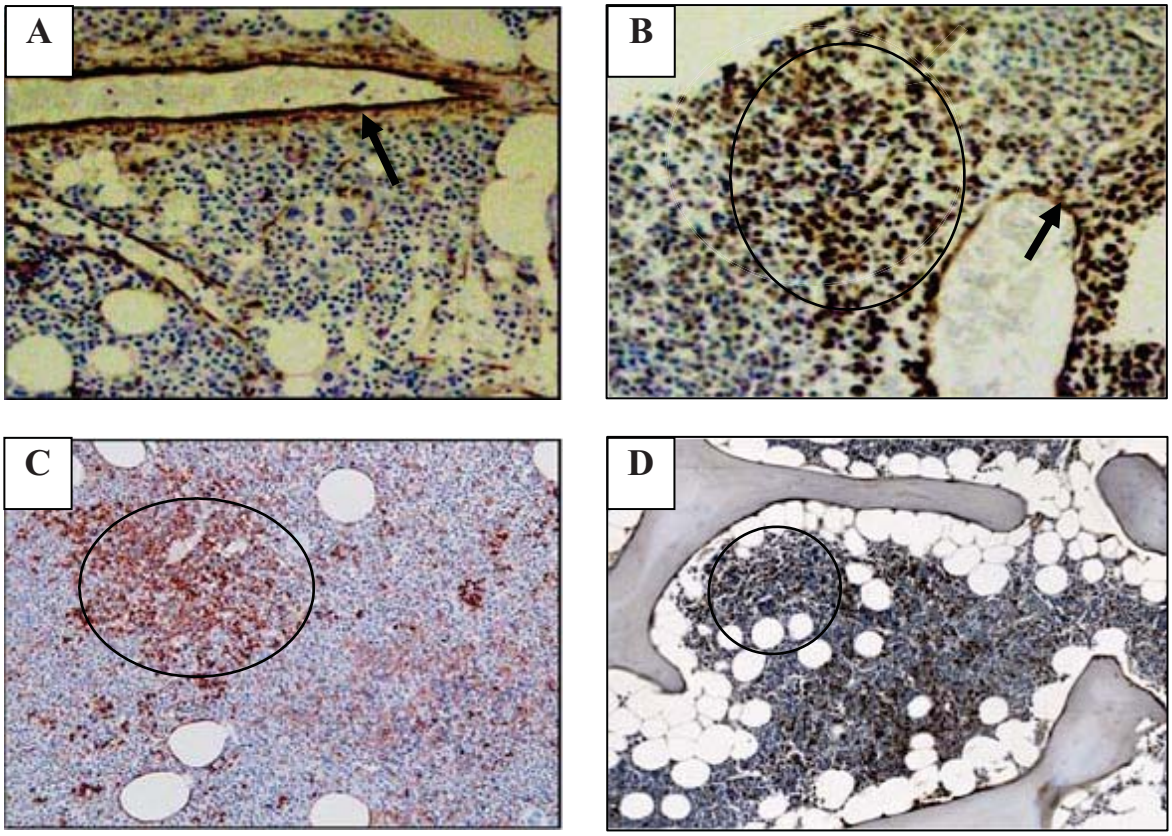
A
B
C
D

Figure 3.6. Circulating Levels of CXCL12 are Elevated in the Peripheral Blood Plasma of MM Patients Compared to MGUS Patients and Normal Donors. The level of CXCL12 in samples of peripheral blood plasma collected from MM (n=62) and MGUS (n=25) patients and age-matched normal donors (n=29) were measured using a CXCL12 ELISA. In (**A**), the CXCL12 plasma concentration for individual patients within the MM, MGUS and control groups is plotted as a dot to illustrate the range in CXCL12 expression observed within each group. In (**B**), the average CXCL12 level for all subjects within each patient group is plotted to illustrate the overall trend in circulating CXCL12 levels between patient groups. Error bars represent the standard error within each cohort of patients. A statistically significant increase in the level of CXCL12 in the peripheral blood circulation was observed in MM patients compared to normal, age-matched donors ($p<0.001$, one-way ANOVA). Whilst an increase in circulating levels of CXCL12 was observed between both MGUS and MM and control and MGUS groups, these differences were not statistically significant ($p=0.16$ and $p=0.06$ respectively, one-way ANOVA).

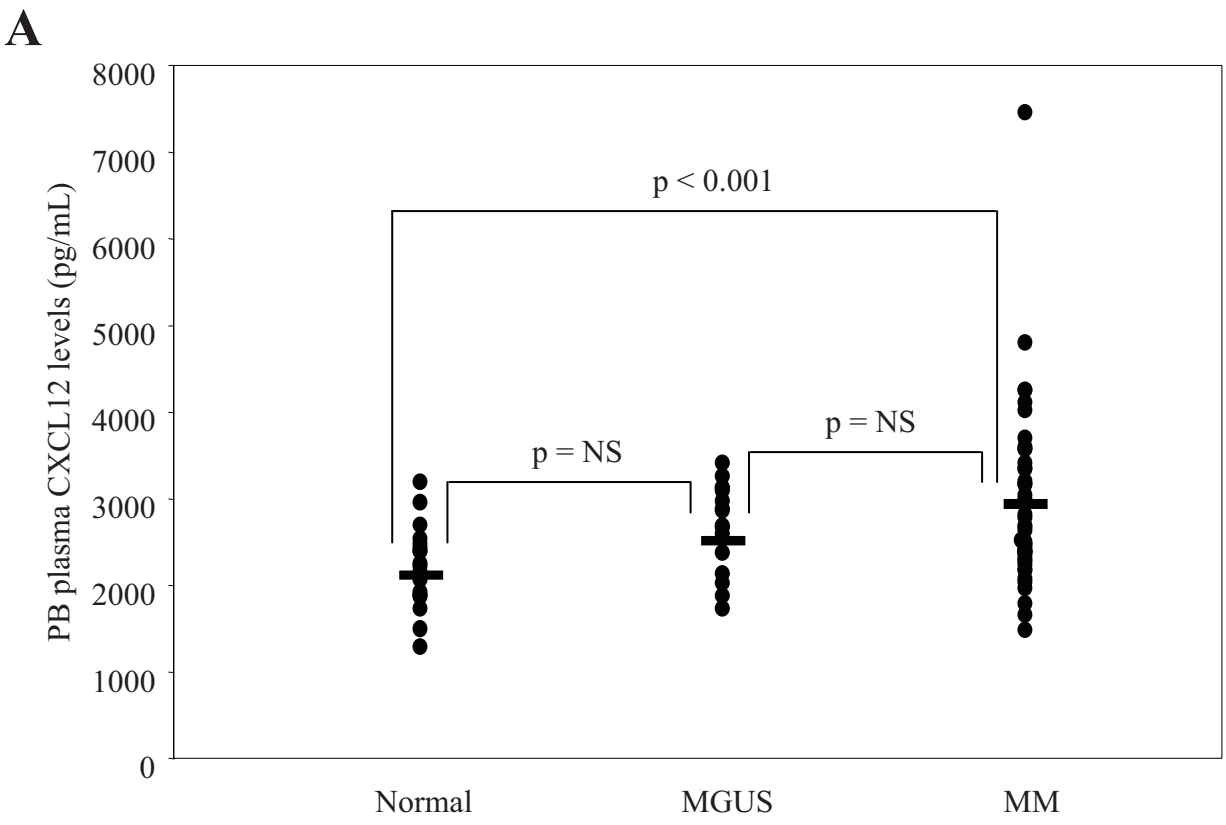
A
8000
7000
6000
5000
4000
3000
2000
1000
0
PB plasma CXCL12 levels (pg/mL)
p < 0.001
p = NS
p = NS
Normal
MGUS
MM

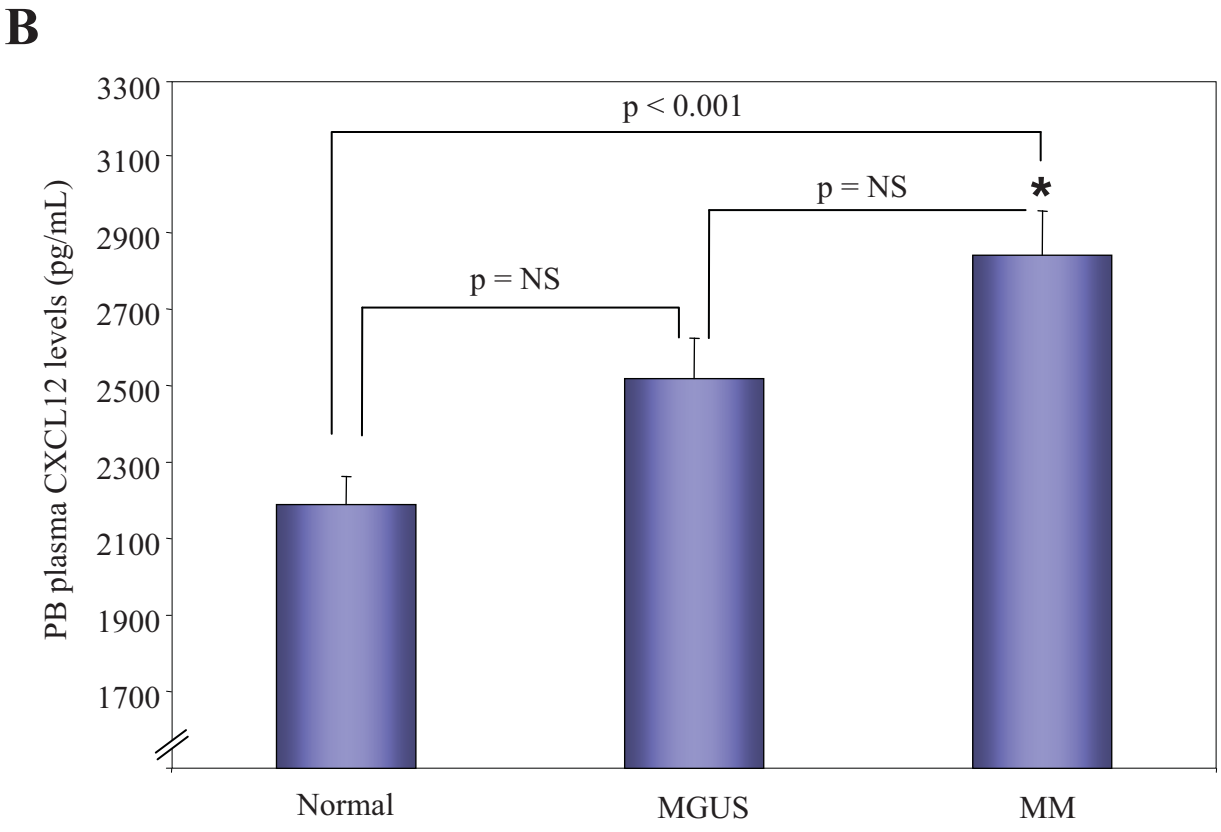
B
3300
3100
2900
2700
2500
2300
2100
1900
1700
PB plasma CXCL12 levels (pg/mL)
p < 0.001
p = NS
p = NS
*
Normal
MGUS
MM

between the MM PC burden and circulating levels of CXCL12. To do this, the PB plasma levels of CXCL12 in MM (n=60) and MGUS (n=26) patients were plotted with reference to their respective BM MM PC burden. A statistically significant correlation was observed between circulating CXCL12 levels and BM PC burden in these MM and MGUS patients (Figure 3.7, $p<0.02$, Pearson Product Moment). Haematologically normal individuals were not included in this assessment because malignant PCs are not present in sufficient numbers in the BM of these subjects.

To test the hypothesis that the elevated CXCL12 in MM patients is involved with angiogenesis, the relationship between circulating CXCL12 levels and BM angiogenesis was examined. In patients where both PB plasma and suitable BM trephine specimens were available, circulating CXCL12 levels from MM (n=35), MGUS (n=15) and age-matched haematologically normal donors (n=6) were plotted with reference to their respective BM MVD measurement. A statistically significant correlation was observed between BM MVD and circulating levels of CXCL12 (Figure 3.8, $p<0.02$, Pearson Product Moment).

3.2.2 *In vitro* Studies

3.2.2.1 HUVECs and TrHBMECs express the CXCR4 receptor.

Having demonstrated a significant association between circulating CXCL12 levels and BM angiogenesis in MM and MGUS patients, the angiogenic properties of CXCL12 were next examined using an established *in vitro* angiogenesis assay. For this assay, two different EC sources were utilised. Firstly, primary HUVECs, derived from neonatal umbilical cords, were used because they are a readily available source of mature primary ECs commonly used in *in vitro* angiogenesis assays [12,417,418]. The second source of ECs was a transformed human BM EC line (TrHBMEC) [419,420], which was considered to be a more tissue-relevant source of EC for these studies.

In order to examine the angiogenic properties of CXCL12 *in vitro*, it was necessary to first confirm that these EC types express the CXCL12 receptor, CXCR4. To do this, total RNA was collected from cultured HUVECs and TrHBMECs and the relative level of *CXCR4* mRNA expression examined using real-time PCR. These data were normalised to the standard housekeeping gene, *GAPDH*, and plotted in Figure 3.9A. Surprisingly, the level of CXCR4 detected in the TrHBMEC line was relatively low compared to the levels

Figure 3.7. Bone Marrow Plasma Cell Burden Correlates with Circulating Levels of CXCL12 in MM and MGUS Patients. The level of CXCL12 in samples of peripheral blood plasma collected from MM (● , n=60) and MGUS (● , n=26) patients at diagnosis were measured using an ELISA and plotted with reference to their respective bone marrow plasma cell burden, as assessed by a haematologist. Haematologically normal individuals were not included in this assessment because malignant PCs are not present in sufficient numbers in the BM of these subjects. Increasing circulating levels of CXCL12 were correlated with increasing plasma cell burden in these MM and MGUS patients, and this was found to be statistically significant ($p<0.02$, Pearson Product Moment).

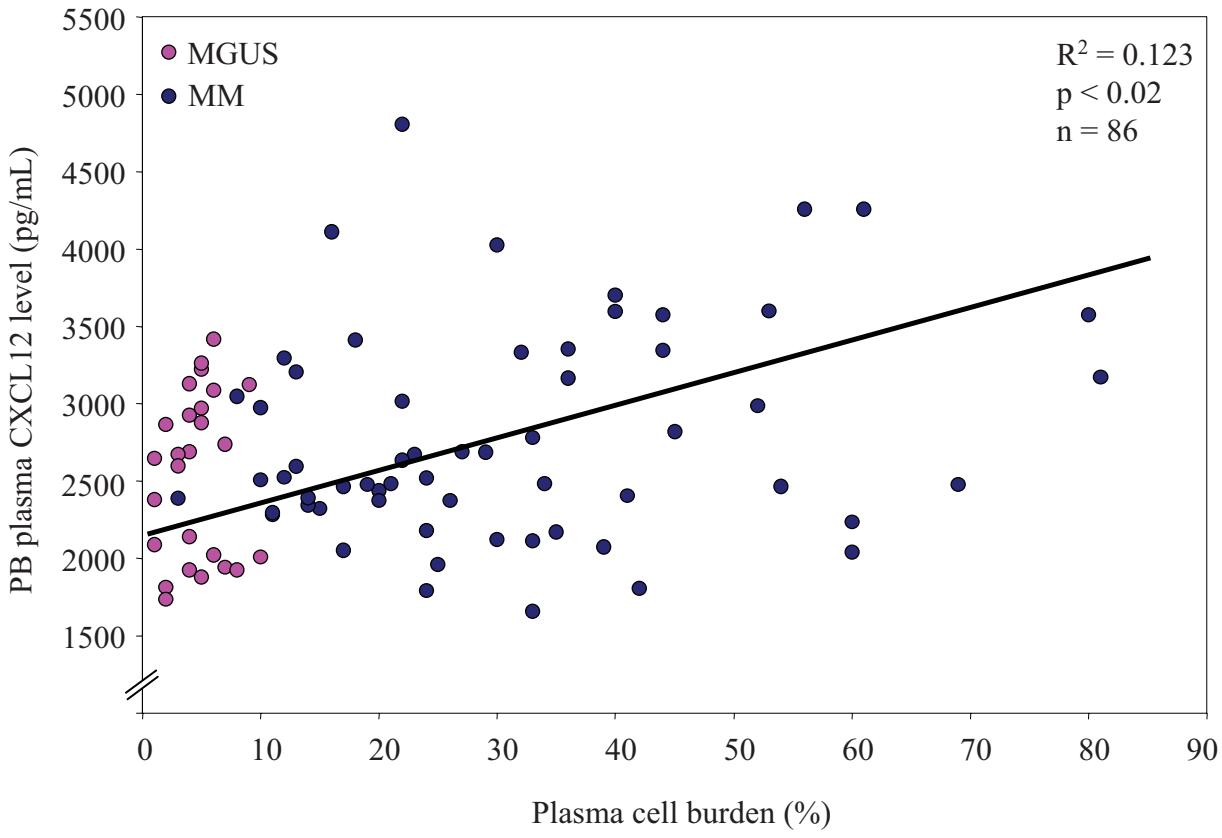
MGUS
MM
$R^2 = 0.123$
$p < 0.02$
$n = 86$
PB plasma CXCL12 level (pg/mL)
5500
5000
4500
4000
3500
3000
2500
2000
1500
0
10
20
30
40
50
60
70
80
90
Plasma cell burden (%)

Figure 3.8. Bone Marrow Microvessel Density Positively Correlates with Circulating Levels of CXCL12 in MM and MGUS Patients and Normal Donors. In patients where both peripheral blood plasma and suitable bone marrow trephine specimens were available, the circulating level of CXCL12 in MM (●, n=35) and MGUS (●, n=15) patients and age-matched normal donors (●, n=6) was measured using an ELISA and plotted with reference to their respective bone marrow microvessel density measurement. Increasing circulating levels of CXCL12 were positively associated with increasing microvessel density, and this correlation was statistically significant ($p<0.02$, Pearson Product Moment).

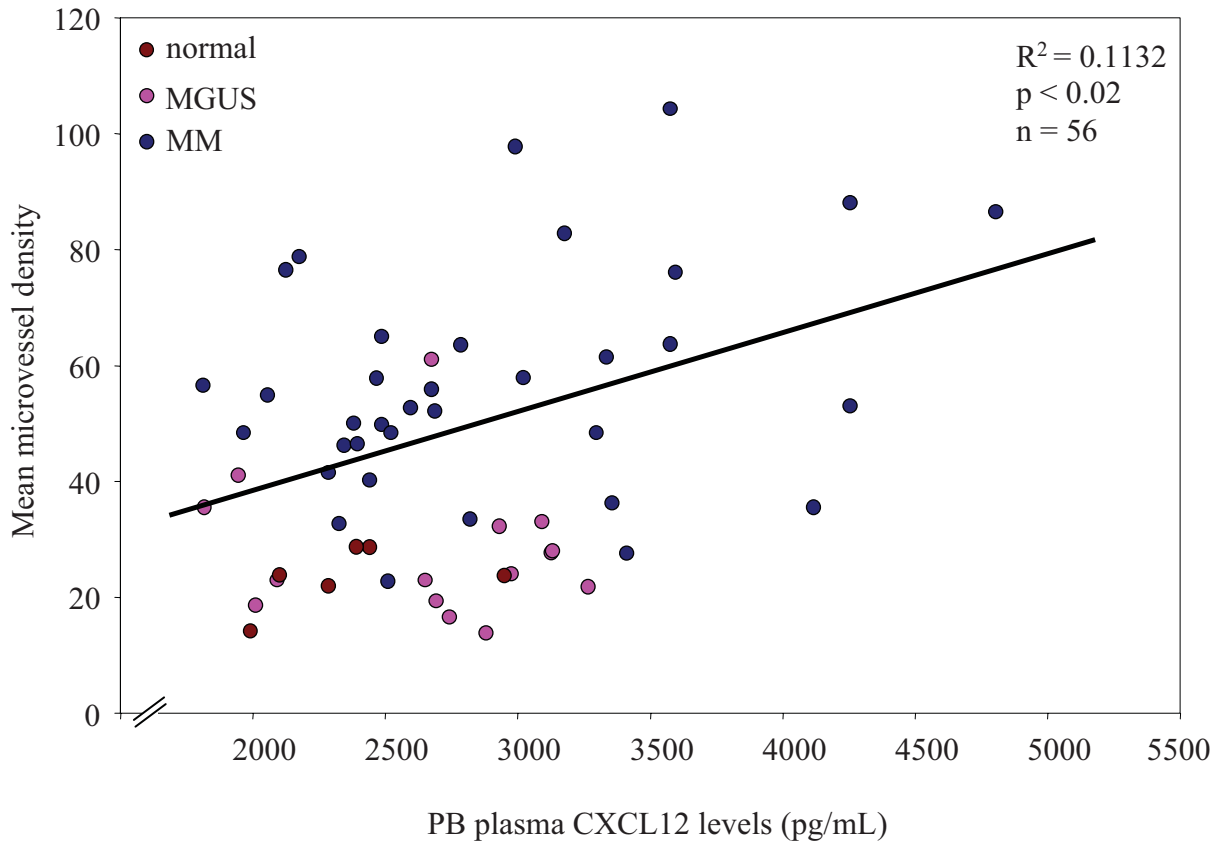
normal
MGUS
MM
$R^2 = 0.1132$
$p < 0.02$
$n = 56$
Mean microvessel density
PB plasma CXCL12 levels (pg/mL)
0
20
40
60
80
100
120
2000
2500
3000
3500
4000
4500
5000
5500

Figure 3.9. CXCR4 Expression on HUVECs and TrHBMECs. (**A**) Levels of *CXCR4* mRNA expression in two primary HUVEC donors and the TrHBMEC line were measured using real-time PCR, and data were normalised to the standard housekeeping gene, *GAPDH*. To better display the lower level of *CXCR4* expression in TrHBMECs, the HUVEC graphs have been truncated and the true values displayed above. Error bars represent the standard error of the mean. (**B** and **C**) HUVECs and TrHBMECs were stained with an anti-CXCR4 monoclonal antibody and its corresponding isotype-matched negative control, and levels of CXCR4 protein expression examined using flow cytometry. Filled histograms (■) indicate levels of background fluorescence following staining with the isotype-matched negative control antibody, and unfilled histograms (▨) represent levels of CXCR4 protein expression in HUVECs and TrHBMECs. The mean fluorescence intensity for each stain is displayed above each histogram, and representative data from three individual experiments using different HUVEC donors and different TrHBMEC cultures is shown.

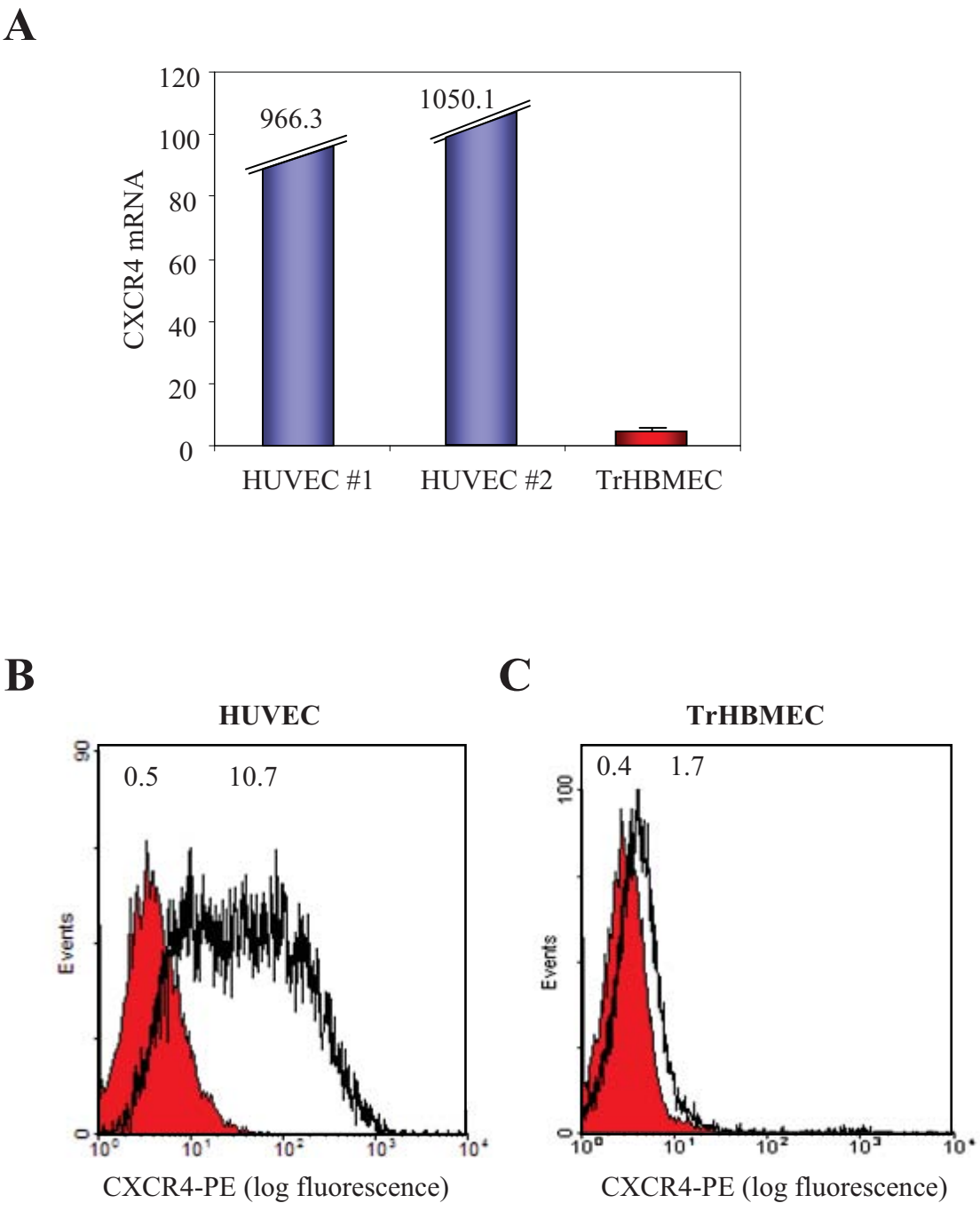
A
120
100
80
60
40
20
0
CXCR4 mRNA
966.3
1050.1
HUVEC #1
HUVEC #2
TrHBMEC
B
HUVEC
0.5
10.7
Events
CXCR4-PE (log fluorescence)
C
TrHBMEC
0.4
1.7
Events
CXCR4-PE (log fluorescence)

observed in primary HUVECs (Figure 3.9A). To extend these real-time PCR studies, cultured HUVECs and TrHBMECs were stained with an anti-CXCR4 monoclonal antibody and levels of cell surface (extracellular) CXCR4 protein expression measured using flow cytometry. In accordance with the real-time PCR data, while HUVECs expressed relatively high levels of CXCR4 protein (Figure 3.9B, mean fluorescence intensity [MFI] =10.7, black line), TrHBMECs were found to express relatively low levels of CXCR4 protein (Figure 3.9C, black line, MFI=1.7). Collectively, these mRNA and protein data confirmed that CXCR4 is expressed by both primary HUVECs and TrHBMEC cells, albeit to different degrees.

3.2.2.2 The effect of recombinant human CXCL12 on in vitro tube formation.

To investigate the angiogenic properties of CXCL12, the ability of recombinant human (rh) CXCL12 to stimulate *in vitro* angiogenesis was investigated using the Matrigel tube formation assay. Preliminary titration experiments were performed to establish the optimal concentration at which rhCXCL12 stimulates *in vitro* tube formation. In these studies, rhCXCL12 was tested at concentrations ranging from 5ng/mL to 500ng/mL for HUVECs (Figure 3.10), and 1ng/mL to 200ng/mL for the TrHBMEC cell line (Figure 3.11). Fifty per cent conditioned media from the RPMI-8226 MM cell line, which contains a potent cocktail of a range of angiogenic factors such as VEGF, bFGF and IL-6, was used in these experiments as a positive control treatment. The respective culture media for HUVECs and TrHBMECs alone were used as a negative control in these experiments.

Using image analysis software, the sum total length of tube networks formed by primary HUVECs in response to each concentration of rhCXCL12 was measured and the data plotted in Figure 3.12A. These data demonstrated that the addition of 50% RPMI-8226 CM to HUVEC cultures stimulated a 3-fold increase in *in vitro* tube formation compared to unstimulated HUVECs alone ($p<0.05$, one-way ANOVA). A dose-dependent increase in HUVEC tube formation was observed in response to increasing concentrations of rhCXCL12. The presence of 200ng/mL rhCXCL12 stimulated robust HUVEC tube formation, and induced a 2.5-fold increase in tube formation compared to untreated cells. While concentrations of rhCXCL12 greater than 100ng/mL induced a statistically significant increase in HUVEC tube formation ($p<0.05$, one-way ANOVA), concentrations in excess of 200ng/mL did not exert any additional effect.

Figure 3.10. The Effect of Recombinant Human CXCL12 on HUVEC *In Vitro* Tube Formation. HUVECs were plated on Matrigel matrix in the presence of (**A**) normal HUVEC medium, or normal HUVEC media supplemented with (**B)** 50% RPMI-8226 conditioned medium, (**C**) 5ng/mL rhCXCL12, (**D**) 30ng/mL rhCXCL12, (**E**) 100ng/mL rhCXCL12, (**F**) 200ng/mL rhCXCL12, (**G**) 300ng/mL rhCXCL12 and (**H**) 500ng/mL rhCXCL12. A dose-dependent increase in *in vitro* angiogenesis was observed in HUVECs treated with rhCXCL12. Digital photographs were taken at x40 magnification following 20 hours of culture and are representative of data from three individual experiments using three different HUVEC donors.

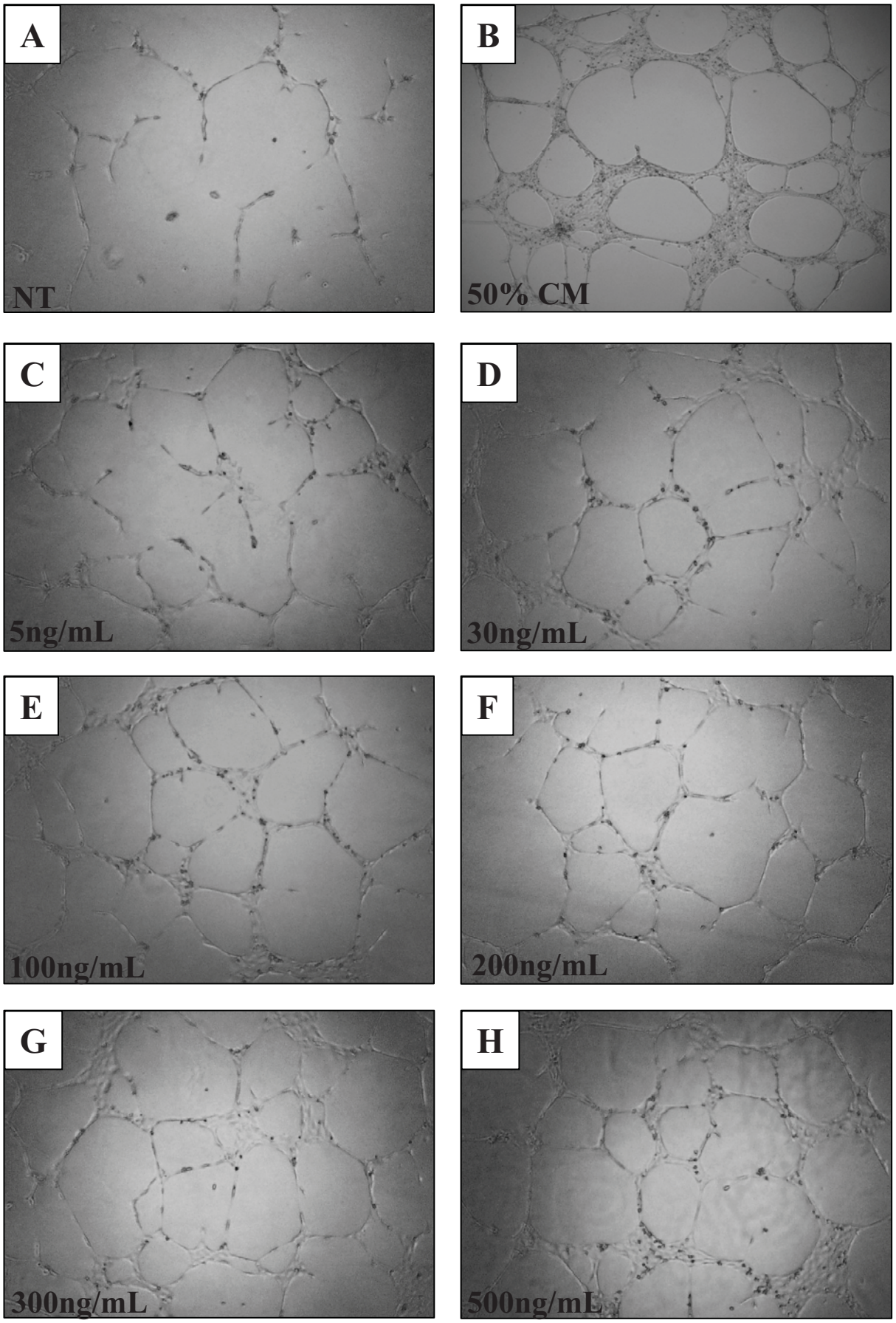
A
NT
B
50% CM
C
5ng/mL
D
30ng/mL
E
100ng/mL
F
200ng/mL
G
300ng/mL
H
500ng/mL

Figure 3.11. The Effect of Recombinant Human CXCL12 on TrHBMEC *In Vitro* Tube Formation. TrHBMECs were plated on Matrigel matrix in the presence of (**A**) normal TrHBMEC medium, or normal TrHBMEC media supplemented with (**B**) 50% RPMI-8226 conditioned medium, (**C**) 1ng/mL rhCXCL12, (**D**) 5ng/mL rhCXCL12, (**E**) 30ng/mL rhCXCL12, (**F**) 50ng/mL rhCXCL12, (**G**) 100ng/mL rhCXCL12 and (**H**) 200ng/mL rhCXCL12. A dose-dependent increase in *in vitro* tube formation was observed in TrHBMECs treated with rhCXCL12. Digital photographs were taken at x40 magnification following 20 hours of culture and representative images from three individual experiments are shown.

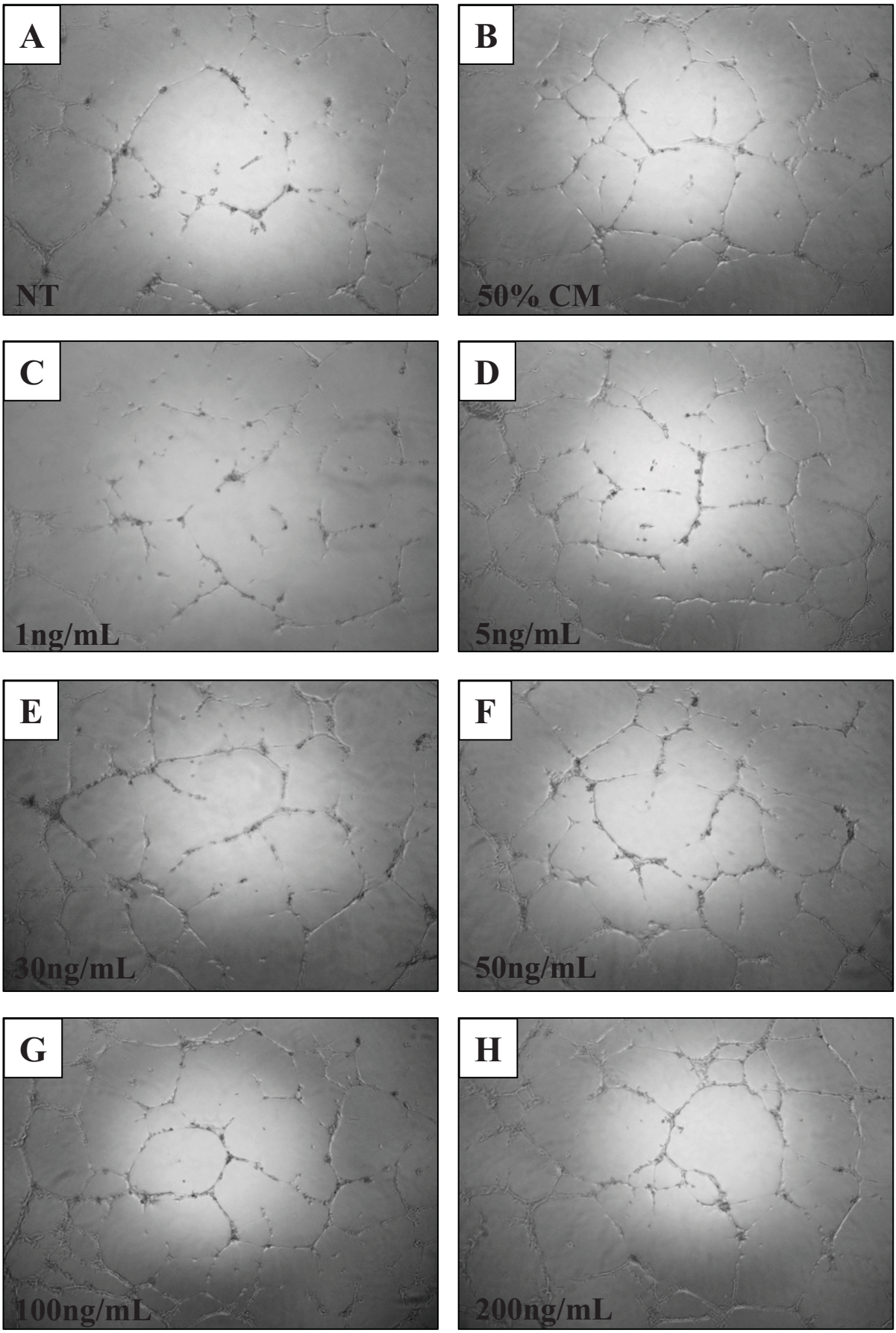
A
NT
B
50% CM
C
1ng/mL
D
5ng/mL
E
30ng/mL
F
50ng/mL
G
100ng/mL
H
200ng/mL

Figure 3.12. Quantitation of The Effect of Recombinant Human CXCL12 on HUVEC and TrHBMEC *In Vitro* Tube Formation. As shown in Figures 3.10 and 3.11, the effect of rhCXCL12 on *in vitro* tube formation was investigated using HUVECs and TrHBMECs. Fifty per cent conditioned media from the RPMI-8226 MM cell line was used as a positive control treatment. Digital photographs taken at x40 magnification of replicate wells following 20 hours of culture were analysed using image analysis software, to determine the sum total length of the tube networks formed per well in response to each concentration of rhCXCL12. Quantitation of these data demonstrated a dose-dependent increase in *in vitro* tube formation in response to rhCXCL12 using both (**A**) HUVECs and (**B**) the TrHBMEC cell line, with 200ng/mL rhCXCL12 found to be the optimal concentration for HUVECs and 30ng/mL for TrHBMECs in this assay system. Data are expressed as mean ± SEM from replicate wells of a representative experiment of three. *$p<0.05$, one-way ANOVA.

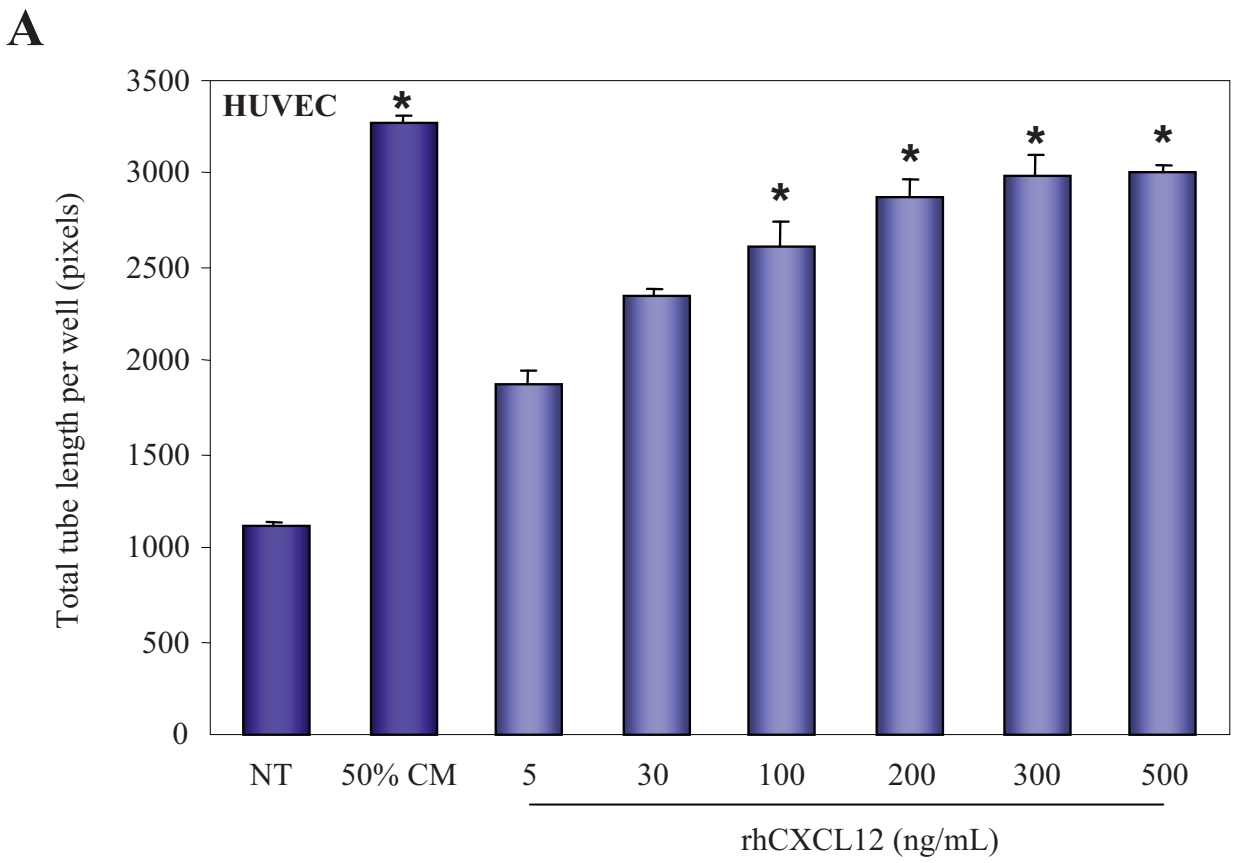
A
HUVEC
Total tube length per well (pixels)
3500
3000
2500
2000
1500
1000
500
0
NT
50% CM
5
30
100
200
300
500
rhCXCL12 (ng/mL)

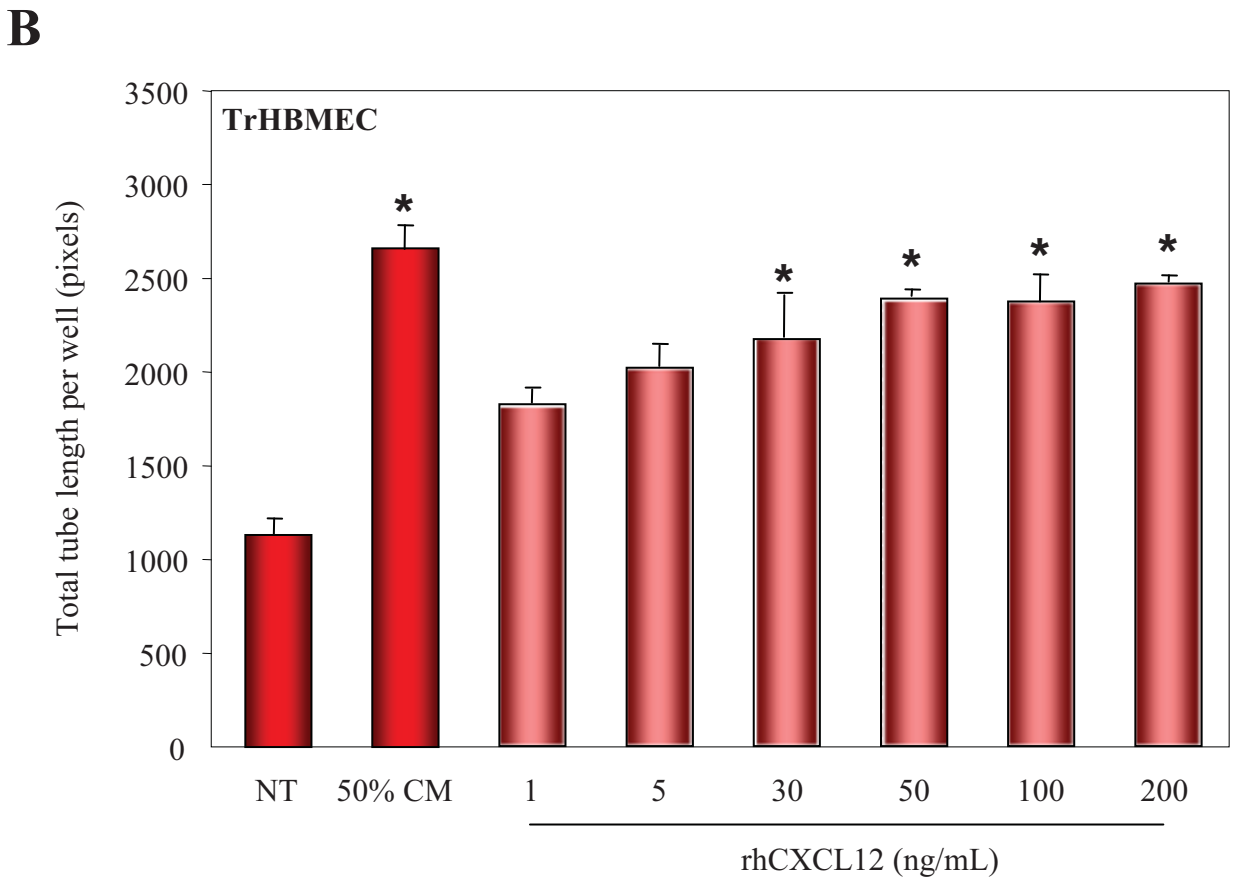
B
TrHBMEC
Total tube length per well (pixels)
3500
3000
2500
2000
1500
1000
500
0
NT
50% CM
1
5
30
50
100
200
rhCXCL12 (ng/mL)

Similarly, the sum total length of tube networks formed by TrHBMECs in response to each concentration of rhCXCL12 was measured and the data plotted in Figure 3.12B. These data showed that the addition of 50% RPMI-8226 CM to TrHBMEC cultures stimulated a 2.4-fold increase in *in vitro* tube formation compared to untreated TrHBMECs alone ($p<0.05$, one-way ANOVA). A dose-dependent increase in TrHBMEC tube formation was also observed in response to increasing concentrations of rhCXCL12, however maximal tube formation was observed at lower concentrations of rhCXCL12 in TrHBMECs than in HUVECs. The presence of 50ng/mL rhCXCL12 and above stimulated robust tube formation in TrHBMECs, inducing a 2-fold increase in tube formation observed compared to untreated cells. While concentrations of rhCXCL12 greater than 30ng/mL induced a statistically significant increase in TrHBMEC tube formation ($p<0.05$, one-way ANOVA), concentrations in excess of 50ng/mL did not exert any additional effect.

3.2.2.3 Myeloma cell line expression of CXCL12.

Having established that rhCXCL12 is a potent stimulator of *in vitro* tube formation in both primary HUVECs and the TrHBMEC cell line, the ability of MM-derived CXCL12 to stimulate *in vitro* tube formation was next examined. To identify a suitable source of MM-derived CXCL12, levels of CXCL12 mRNA and protein expression in eight human MM PC lines were measured using real-time PCR and ELISA, respectively.

Total RNA samples were harvested from the RPMI-8226, U266, JIMI, LP-1, NCI-H929, OPM-2 and WL2 cell lines and from two samples of $CD38^{+++}$ MACs-selected MM PCs derived from the BM of MM patients. Using real-time PCR, the level of *CXCL12* mRNA expression in these samples was examined, and data normalised to the expression of the standard housekeeping gene, *GAPDH* (Figure 3.13A). Highly variable levels of *CXCL12* mRNA expression were observed between each of the MM cell lines compared to the patient-derived $CD38^{+++}$ PCs. Insignificant levels of *CXCL12* expression were detected in JIMI, NCI-H929, OPM-2 and WL2 cell lines, and relatively modest levels detected in the U266 and LP-1 cell lines and patient-derived $CD38^{+++}$ MM PCs. Strikingly, extremely high levels of *CXCL12* expression were detected in RPMI-8226 cells.

In parallel studies, the level of CXCL12 protein expression in each of these eight MM cell lines was also examined (Figure 3.13B). Following 72 hours of culture, supernatant was collected from each cell line and CXCL12 levels measured using an ELISA. CXCL12

Figure 3.13. CXCL12 Expression in Myeloma Cell Lines. (**A**) Using real-time PCR, levels of *CXCL12* mRNA expression were measured in a range of myeloma cell lines (RPMI-8226, U266, JIMI, LP-1, NCI-H929, OPM-2 and WL2) and samples of purified MM patient-derived $CD38^{+++}$ plasma cells. Data were normalised to the standard housekeeping gene, *GAPDH*. To better display the lower expression levels of *CXCL12* mRNA in the majority of cell lines tested, the RPMI-8226 graph has been truncated and the true value displayed above. Error bars represent the standard error within each group. (**B**) Levels of CXCL12 protein expression were measured in conditioned media from the myeloma cell lines or MM patient-derived peripheral blood plasma samples using a CXCL12 ELISA. Graphical representation of these data illustrates CXCL12 protein concentration in the conditioned media collected from each cell line, normalised to total cellular protein concentration, and demonstrates that essentially all myeloma cell lines tested expressed appreciable levels of CXCL12 protein. To better display the lower expression levels of CXCL12 in these cell line samples, the patient-derived plasma cell graphs have been truncated and the true value displayed above. Error bars represent the standard error within each group.

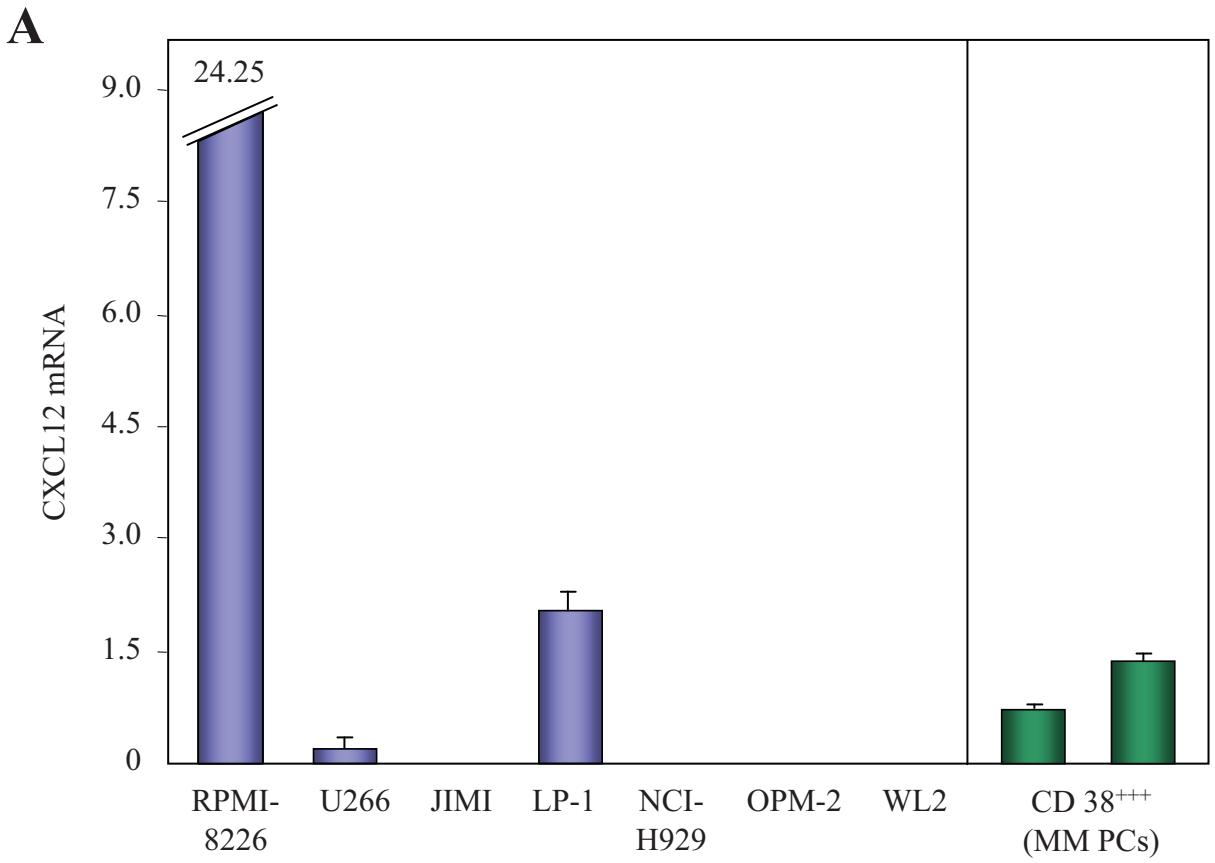
A
24.25
9.0
7.5
6.0
4.5
3.0
1.5
0
CXCL12 mRNA
RPMI-8226
U266
JIMI
LP-1
NCI-H929
OPM-2
WL2
CD 38+++ (MM PCs)

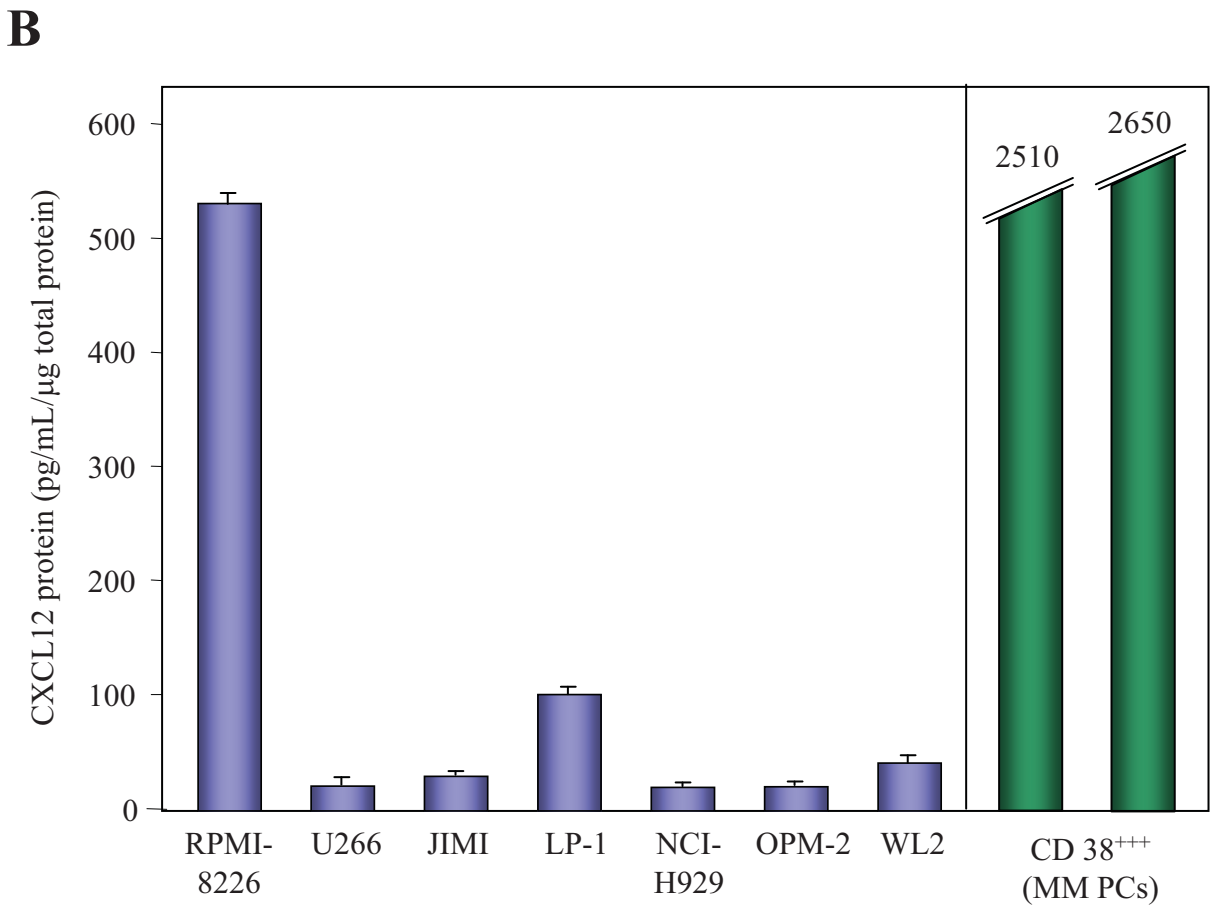
B
600
500
400
300
200
100
0
CXCL12 protein (pg/mL/µg total protein)
2510
2650
RPMI-8226
U266
JIMI
LP-1
NCI-H929
OPM-2
WL2
CD 38+++ (MM PCs)

protein expression was assessed after 72 hours to maximise time for CXCL12 "conditioning" of the medium. In order to account for any differences in the proliferation rates of these cell lines, data were normalised to the total protein content of the cells from which each supernatant was collected. As a point of reference, CXCL12 levels were also measured in PB plasma samples from MM patients. While variable in magnitude, essentially all MM cell lines expressed CXCL12 protein. The supernatants collected from the U266, JIMI, NCI-H929, OPM-2 and WL2 cell lines each contained relatively low levels of CXCL12 protein, with concentrations of less than 50pg/mL detected. The supernatant from the LP-1 and RPMI-8226 cell lines contained appreciable levels of CXCL12 protein, with concentrations of 103.1 ± 9.1pg/mL and 509.8 ± 15.2 pg/mL detected, respectively. Strikingly, compared to all of the cell line supernatants, extremely high levels of CXCL12 protein were detected in patient-derived PB plasma samples. On the basis of these mRNA and protein analyses, the RPMI-8226 cell line was found to express levels of CXCL12 most similar to that of patient-derived $CD38^{+++}$ MM PCs and was chosen as the most representative source of MM-derived CXCL12.

3.2.2.4 Inhibition of the CXCL12-CXCR4 pathway partially reduces myeloma-induced angiogenesis.

As demonstrated earlier, the RPMI-8226 MM cell line expresses CXCL12 at levels comparable to that found in patient samples (see Figure 3.13). To investigate the angiogenic properties of MM-derived CXCL12, the ability of RPMI-8226 CM to stimulate *in vitro* angiogenesis was investigated using the Matrigel tube formation assay. Based on previous comparative studies of primary HUVECs and the TrHBMEC line (see Sections 3.2.2.1 and 3.2.2.2), HUVECs were chosen for all assays described hereafter on the basis of greater reproducibility and the capacity to induce more robust tube formation. Preliminary titration experiments using primary HUVECs were performed using various concentrations of RPMI-8226 CM ranging from 5% to 50%, and unstimulated HUVECs cultured in their normal medium alone were used as a negative control (Figure 3.14).

Using image analysis software, the sum total length of tube networks formed by HUVECs in response to each concentration of RPMI-8226 CM was measured and plotted in Figure 3.15. These data demonstrate that RPMI-8226 CM stimulates a dose-dependent increase in *in vitro* tube formation. The presence of 20% CM stimulated a 2-fold increase in tube

Figure 3.14. The Effect of RPMI-8226 CM on *In Vitro* Tube Formation. HUVECs were plated on Matrigel matrix in the presence of (**A**) normal HUVEC medium, or normal HUVEC media supplemented with (**B**) 5% RPMI-8226 CM, (**C**) 10% RPMI-8226 CM, (**D**) 20% RPMI-8226 CM, or (**E**) 50% RPMI-8226 CM. Digital photographs were taken at x40 magnification following 20 hours of culture and representative images from three individual experiments performed using three different HUVEC donors are shown.

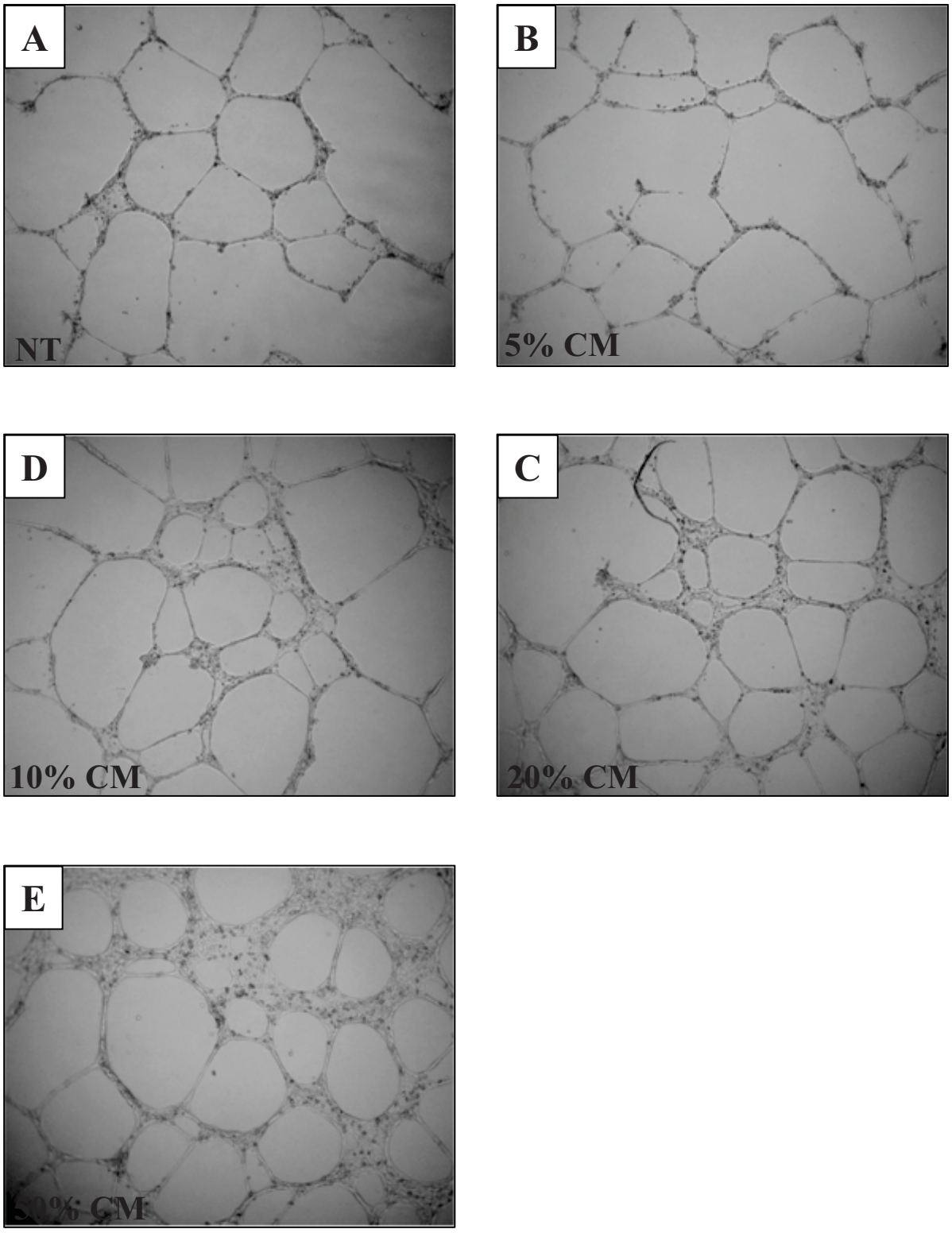
A
NT
B
5% CM
D
10% CM
C
20% CM
E

Figure 3.15. Quantitation of The Effect of RPMI-8226 CM on *In Vitro* Tube Formation. As shown in Figure 3.14, the effect of RPMI-8226 CM on *in vitro* tube formation was investigated using various concentrations of CM. Digital photographs taken at x40 magnification of replicate wells following 20 hours of culture were analysed using image analysis software, to determine the sum total length of the tube networks formed per well in the presence of each treatment. Quantitation of these data demonstrated a dose-dependent increase in CM-mediated tube formation, with 20% and 50% concentrations stimulating a statistically significant increase compared to unstimulated HUVECs (*$p<0.05$ and **$p< 0.001$, one-way ANOVA). Data are expressed as mean ± SEM from replicate wells of a representative experiment of three.

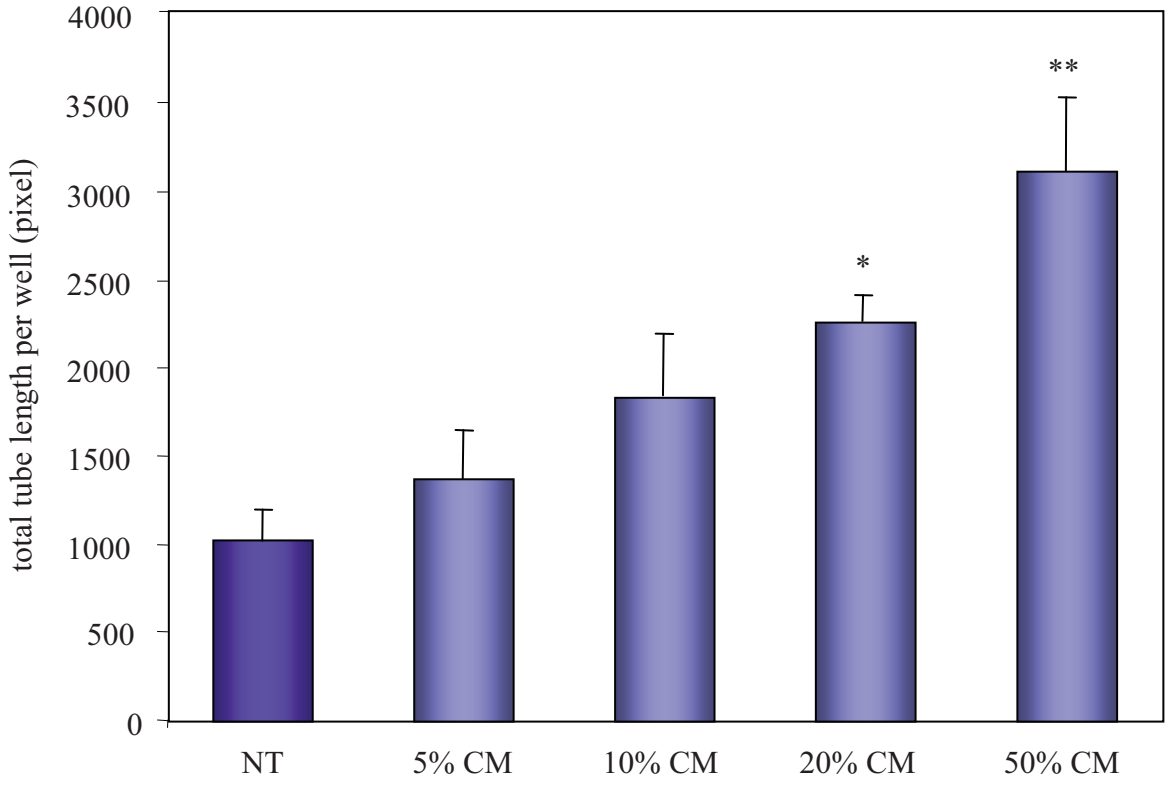
4000
3500
3000
2500
2000
1500
1000
500
0
total tube length per well (pixel)
**
*
NT
5% CM
10% CM
20% CM
50% CM

formation compared to unstimulated HUVECs alone ($p<0.05$, one-way ANOVA), and 50% CM induced a 3-fold increase in *in vitro* tube formation ($p<0.001$, one-way ANOVA). Whilst the presence of 5% and 10% CM also stimulated *in vitro* tube formation, these effects were not statistically significant ($p=0.9$ and $p=0.34$ respectively, one-way ANOVA).

To investigate the contribution of MM-derived CXCL12 in the increased tube formation observed in the presence of RPMI-8226 CM, tube formation assays were performed using 50% CM in the presence of the CXCR4 antagonist, 4F-Benzoyl-TE14011 (T140). T140 is a potent small-molecule inhibitor which binds to the CXCR4 receptor with high affinity, thereby preventing the binding of CXCL12. HUVECs were pre-incubated with either 1μM or 5μM T140 on ice for 30 minutes prior to the addition of the respective treatments, in order to ensure that all CXCR4 receptors were occupied by the antagonist and therefore rendered non-responsive to CXCL12 within the CM. As a negative control, unstimulated HUVECs were also cultured in the presence or absence of either 1μM or 5μM T140 (Figure 3.16).

Using image analysis software, the sum total length of tubes formed in response to each of these treatments was measured and the data plotted in Figure 3.17. These data demonstrated that the addition of RPMI-8226 CM stimulated a 3-fold increase in *in vitro* tube formation compared to unstimulated HUVECs alone. Importantly, the addition of 1μM and 5μM T140 mediated a 35 - 40% reduction in the total length of tube networks formed in response to 50% RPMI-8226 CM ($p<0.001$, one-way ANOVA). In the absence of RPMI-8226 CM, the T140 antagonist had no effect on tube formation, confirming that the reduction in CM-mediated tube formation observed in response to T140 was not due to a non-specific or toxic effect.

Figure 3.16. The Effect of MM-derived CXCL12 on *In Vitro* Tube Formation. HUVECs were plated on Matrigel matrix in the presence of (**A**) normal HUVEC medium, or normal HUVEC media supplemented with (**B**) 50% RPMI-8226 CM, (**C**) 50% RPMI-8226 CM + 1μM T140 (CXCR4 antagonist), or (**D**) 50% RPMI-8226 CM + 5μM T140 (CXCR4 antagonist). Digital photographs were taken at x40 magnification following 20 hours of culture and representative images from three individual experiments performed using three different HUVEC donors are shown.

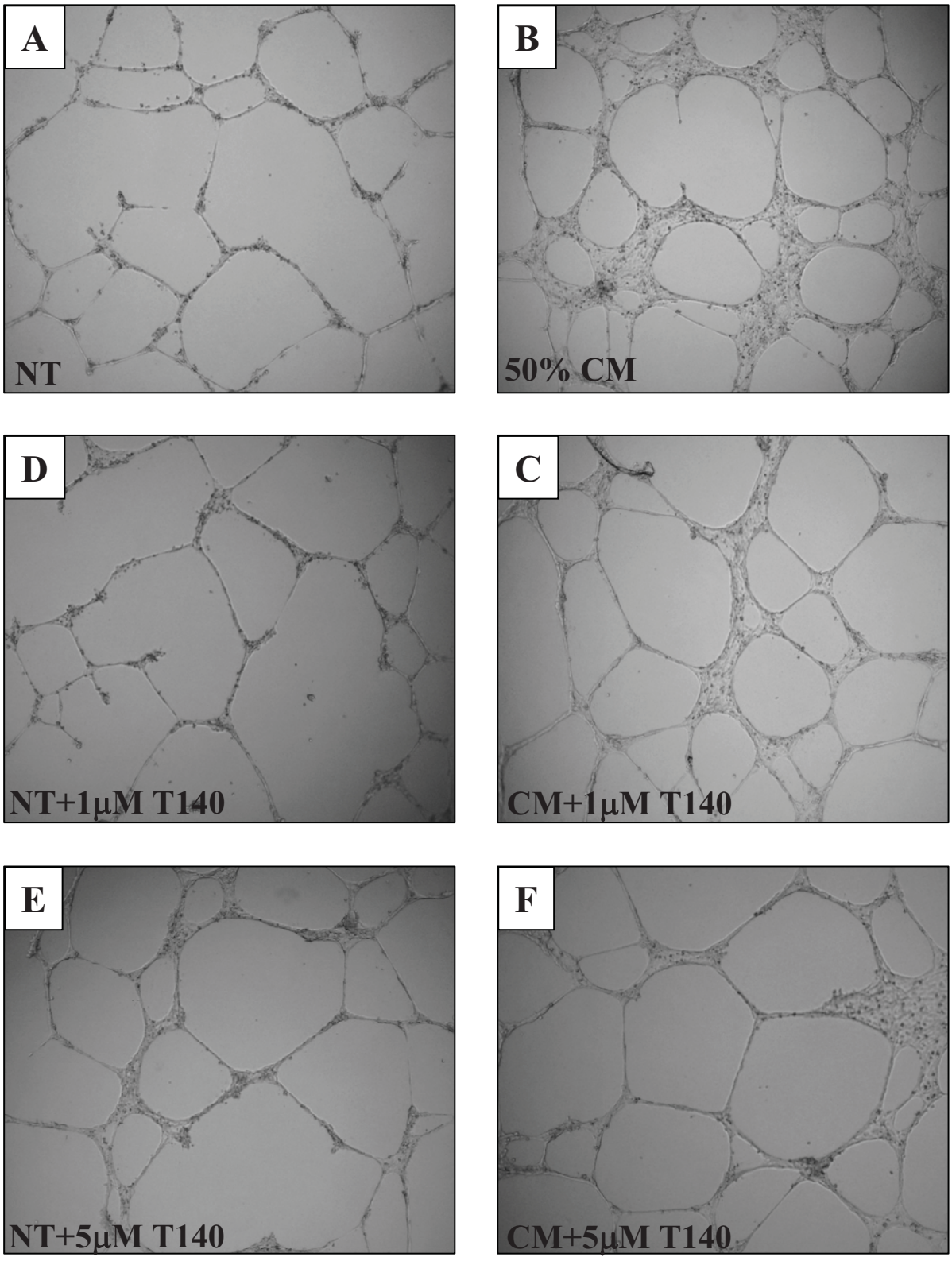
A
NT
B
50% CM
D
NT+1μM T140
C
CM+1μM T140
E
NT+5μM T140
F
CM+5μM T140

Figure 3.17. Quantitation of The Effect of MM-derived CXCL12 on *In Vitro* Tube Formation. As shown in Figure 3.16, the effect of MM-derived CXCL12 on *in vitro* tube formation was investigated using conditioned media from the RPMI-8226 myeloma cell line in the presence or absence of the CXCR4 inhibitor, T140. As a negative control, T140 was also added to unstimulated cells. Digital photographs taken at x40 magnification of replicate wells following 20 hours of culture were analysed using image analysis software, to determine the sum total length of the tube networks formed per well in the presence of each treatment. Quantitation of these data demonstrated a significant reduction in CM-mediated tube formation in the presence of both concentrations of T140 (1μM and 5μM, $p<0.001$, one-way ANOVA). Data are expressed as mean ± SEM from replicate wells of a representative experiment of three.

*$p<0.001$, compared to respective treatment in the absence of antagonist, one-way ANOVA.

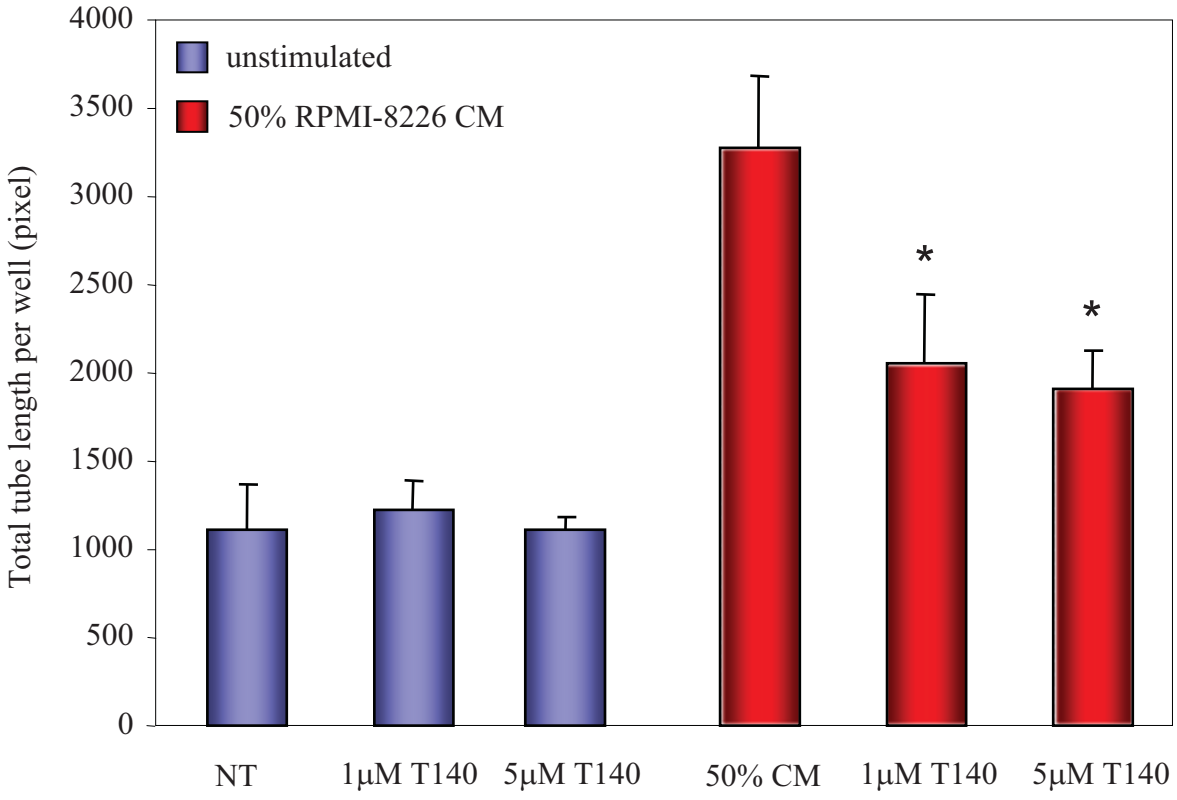
4000
3500
3000
2500
2000
1500
1000
500
0
Total tube length per well (pixel)
unstimulated
50% RPMI-8226 CM
*
*
NT
1μM T140
5μM T140
50% CM
1μM T140
5μM T140

3.3 Summary and Discussion

Angiogenesis is a hallmark of tumour progression in solid and haematological cancers, and provides tumour cells with an adequate blood supply to facilitate tumour growth and metastasis. In MM, the molecular mechanisms responsible for the progressive increase in BM angiogenesis remain uncertain, due to the complexity of interactions between tumour cells and host cells, and the secretion of an array of pro-angiogenic chemokines, cytokines, growth factors and enzymes. Previous studies have shown that CXCR4 is expressed by ECs, and that CXCL12 is a potent EC chemoattractant [10,177,178]. However, despite recent reports demonstrating that CXCL12 is a potent angiogenic chemokine [10,12,253] and that MM PCs are an abundant source of CXCL12 in the BM [9], its role in angiogenesis in MM has yet to be examined. In this chapter, the role of CXCL12 in promoting angiogenesis was examined in MM patient samples and in *in vitro* tube formation assays.

MVD assessment is a widely-used diagnostic tool to measure angiogenesis in cancer and correlates with disease parameters such as overall survival, tumour metastasis, and response to therapy [421]. MVD assessment reflects the intercapillary distance between neighbouring vessels, which is determined by numerous interrelated local factors including the metabolic requirements of resident cells and the net balance between angiogenic and angiostatic stimuli [422]. Following established methods of MVD assessment on patient BM trephines, studies presented in this chapter confirm previous findings that BM MVD is significantly higher in MM patients compared to healthy individuals and MGUS patients [4,7,8,31,116,412,413].

The contribution of angiogenesis to the development of MGUS remains unclear, as contradictory findings are reported in the literature. While Laroche *et al* [407] and Rajkumar *et al* [413] have reported that MGUS patients have a higher BM MVD than their healthy counterparts, our findings confirm studies performed by De Raeve *et al* [423], who showed that there is no significant difference in BM MVD between healthy individuals and MGUS patients. The reasons for these contradictory results are unknown. While different methods of MVD assessment were used in these investigations, studies presented in this chapter showed no significant difference between the “hot spot” and “whole trephine” method of MVD assessment. Furthermore, the differences cannot be explained by insufficient sample size, as each of these studies was performed on 50 - 400 patients. However, while we are unable to account for these contradictory findings regarding the

BM MVD of MGUS patients compared to healthy individuals in these studies, there is a body of evidence to support our finding that MGUS is a pre-vascular disease state. Using primary PCs from the BM of MM and MGUS patients, Vacca *et al* examined the ability of CM from these cells to induce angiogenesis using the chick embryo chorioallantoic membrane assay. In these studies, 20/26 (76%) of CM samples from active MM patients induced dense capillary growth and a significant increase in microvessel area, whereas an induction of angiogenesis was only observed in 4/20 (20%) of MGUS patient samples [134]. Similarly, Kumar *et al* [41] examined the ability of BM plasma samples from healthy individuals and MGUS and MM patients to induce *in vitro* angiogenesis. In these studies, only 2/30 (7%) of MGUS samples stimulated *in vitro* angiogenesis and 19/30 (63%) actually inhibited angiogenesis [41]. Further investigation found that the BM of healthy individuals and MGUS patients contains predominantly angiostatic factors, the identities of which are currently unknown [41]. In other studies, Dominici *et al* [128] examined the angiogenic "potential" of BM mononuclear cells from normal, MGUS and MM patients by evaluating their ability to form endothelial colonies. In these studies, no difference in endothelial colony formation was observed between normal and MGUS patients [128]. Collectively, these studies suggest that MGUS does not represent an angiogenic disease state.

Having demonstrated that BM MVD is associated with disease progression between MGUS and MM, further analyses were performed to examine whether BM MVD was directly associated with the extent of malignant PC infiltration in the BM. Consistent with previous findings [115,116], we found a direct association between BM PC burden and BM MVD which suggests a direct relationship between MM PC growth and BM angiogenesis. While data contradictory to this was reported by Rajkumar *et al* in 2000[6], their follow-up study with a much larger cohort of patients later showed a direct correlation between BM MVD and BM PC burden [413].

The CXCL12 chemokine is important in many of aspects of MM biology including MM PC homing, transendothelial migration and retention within the BM [164,168,265,266], and osteoclastic bone resorption [9]. In the normal BM environment, CXCL12 is expressed by a number of different cells including OBs lining endosteal surfaces [215,415,416], BMSCs [415], and vascular ECs [415]. Using immunohistochemical techniques to examine CXCL12 expression in patient BM trephine biopsies, studies presented here confirm previous findings from our

laboratory that CXCL12 is strongly expressed by MM PCs in MM patients [9]. Moreover, these studies demonstrate, for the first time, that circulating levels of CXCL12 correlate with the aberrant BM angiogenesis observed in MM and MGUS patients. Interestingly, while the average circulating CXCL12 levels in our cohort of MGUS patients was moderately higher than that of healthy individuals (Figure 3.6), no difference was observed in the average BM MVD between these groups (Figure 3.3). This most likely reflects the sensitivity of measuring circulating CXCL12 levels in the PB. While it would be preferable to measure CXCL12 levels in BM aspirates, in our experience BM is often unavoidably contaminated with blood during collection, which confounds the accuracy of this approach. Nevertheless, using matched PB and trephine samples from our cohort of MM and MGUS patients, the data clearly demonstrates that circulating CXCL12 levels are associated with BM MVD.

The Matrigel tube formation assay is a well-defined *in vitro* assay which is used to investigate the effect of various substances on EC adherence, migration and ability to differentiate into tube-like structures. The key advantage of this assay is the ability to assess an effect on EC activity over a very short time frame. The majority of *in vitro* studies presented here were performed using primary ECs derived from umbilical cords, HUVECs. However, in recognition of the phenotypic differences between ECs throughout the body, a transformed EC line derived from BM ECs (TrHBMEC) [419,420] was also used as a more tissue-relevant source of ECs. Morphologically, obvious differences between primary HUVECs and the transformed TrHBMECs were observed: the TrHBMECs had a slightly more spindle-shaped appearance than HUVECs, the growth rate of the TrHBMECs was considerably faster than that of the primary HUVEC cultures and, while HUVEC growth was contact-inhibited, TrHBMEC cultures were able to grow to higher densities. Previous studies have also demonstrated differences between HUVECs and TrHBMECs in terms of adhesion molecule expression, surface chemokine receptor expression and chemokine production [424].

Interestingly, the TrHBMEC line exhibited markedly lower levels of *CXCR4* mRNA and protein expression than primary HUVECs. This observation was previously reported by Yun *et al* [425] who, despite being able to readily detect CXCR4 protein expression by vascular ECs in human BM specimens, were unable to detect CXCR4 mRNA and protein expression in cultured primary BMECs and the transformed BMEC-1 cell line. The low

levels of CXCR4 expression in TrHBMECs, which is not reflective of the *in vivo* setting, coupled with the finding that TrHBMECs do not form robust tubules like primary HUVECs, led us to discontinue the use of TrHBMECs in our study.

Using CM from the MM PC line, RPMI-8226, MM-derived CXCL12 was found to be a potent stimulator *in vitro* angiogenesis. Previous reports have identified several agents with the ability to selectively block interactions between CXCL12 and CXCR4 both *in vitro* and *in vivo*. These agents include the bicyclam AMD-3100 [426-428], the synthetic peptide polyphemusins T134 [429] and 4F-Benzoyl-TE14011 (T140) [430,431]. T140 and structurally related analogues have been shown to inhibit CXCL12 chemotaxis in a variety of cell types [245,260,432-435], inhibit *in vitro* OC activity and osteolytic bone disease *in vivo* [9], suppresses the delayed-type hypersensitivity response in mice [436], and reduce pulmonary metastasis of breast cancer cells [432]. Using the T140 antagonist, the increase in angiogenesis mediated by RPMI-8226 CM was directly attributed to CXCL12, as the addition of T140 significantly reduced the CM-mediated increase in angiogenesis. Considering that the RPMI-8226 CM would contain a multitude of angiogenic growth factors, the magnitude of T140 inhibition on tube formation in the presence of conditioned medium was surprising. However, this is likely to reflect the fact that in addition to directly acting on EC, MM-derived factors such as VEGF and bFGF act, in part, by up-regulating expression of CXCR4 on ECs [10].

In summary, the studies presented in this chapter have demonstrated that circulating CXCL12 levels are elevated in MM patients compared to MGUS patients and age-matched healthy individuals, and that circulating CXCL12 levels correlate with BM MVD in MM and MGUS patients. Furthermore, recombinant and MM-derived CXCL12 were found to stimulate *in vitro* angiogenesis in the Matrigel tube formation assay. As depicted in Figure 3.18, these findings add to our understanding of the importance of CXCL12 in MM biology and show for the first time that MM-derived CXCL12 induces angiogenesis. We have also shown that the malignant transformation from MGUS to MM, which is associated with the acquisition of an angiogenic phenotype, is associated with increased CXCL12 production by PCs. With the knowledge that high levels of CXCL12 produced by MM PCs promote osteolysis in MM patients [9], these data suggest that inhibition of CXCL12 may be an effective strategy to target multiple aspects of MM biology. However, as MM-induced angiogenesis is a complex process that involves a multitude of cytokines

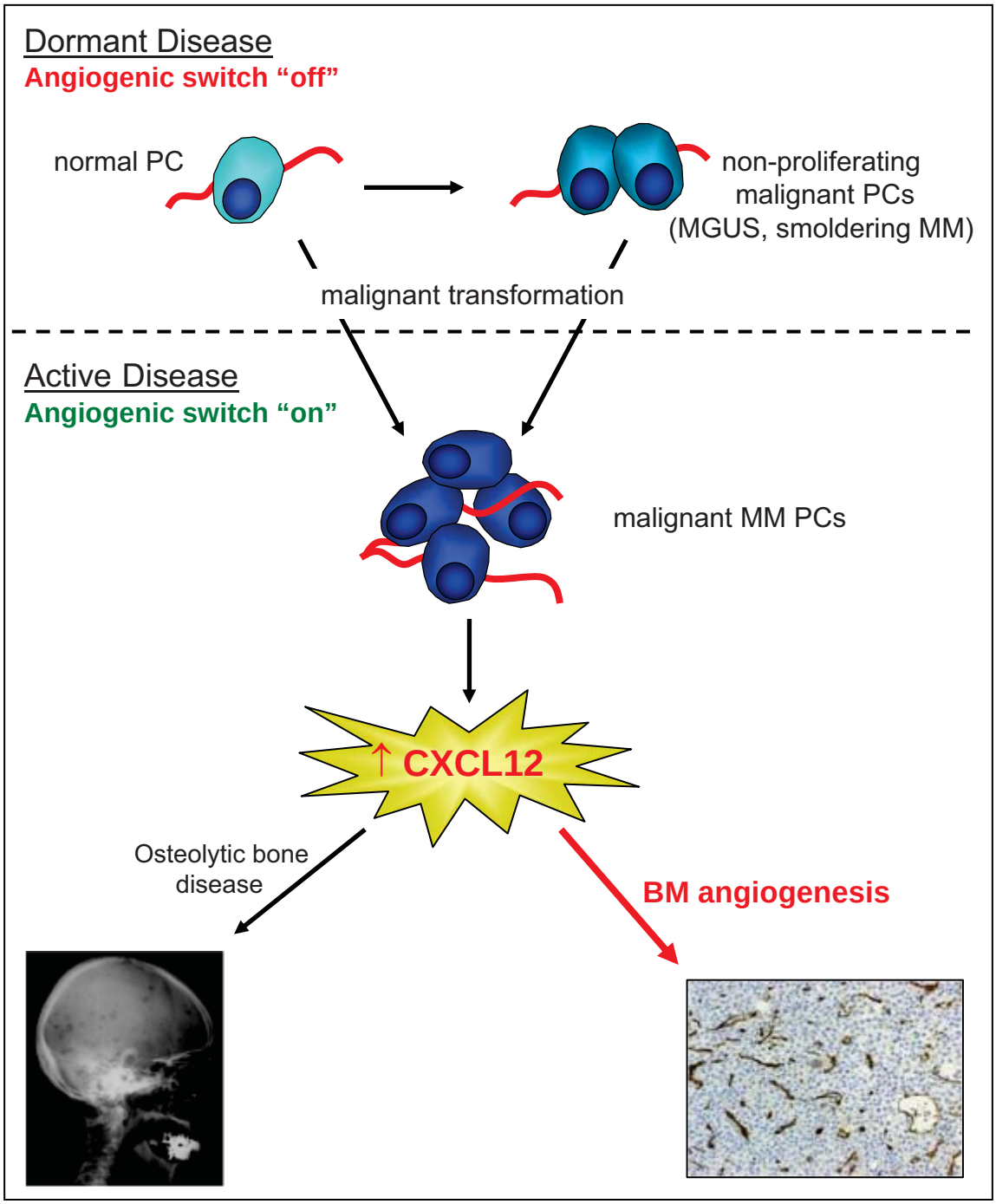

Figure 3.18. Key Findings Arising From This Chapter. The malignant transformation of MM PCs is associated with activation of the angiogenic switch. Following established methods of MVD assessment, studies presented in this chapter have confirmed that BM MVD is significantly higher in MM patients compared to healthy individuals and MGUS patients. Further examination revealed a direct correlation between circulating levels of CXCL12 and BM MVD, and using *in vitro* tube formation assays, MM-derived CXCL12 was found to strongly induce *in vitro* angiogenesis. The CXCL12/CXCR4 axis is important in many aspects of MM biology, and these findings highlight its additional role in mediating BM angiogenesis.

and growth factors, further studies are required to investigate the relationship between CXCL12 and other angiogenic factors in the BM microenvironment. Furthermore, while two dimensional *in vitro* angiogenesis assays such as the Matrigel tube formation assay are informative, they are unable to accurately reproduce the *in vivo* setting because they cannot account for the contribution of microenvironmental cues provided by SMCs, inflammatory cells and stromal cells. To address the deficiencies of *in vitro* assay systems, studies presented in Chapter 5 were performed to examine the role of CXCL12 in mediating angiogenesis in an *in vivo* mouse model.